Hydraulic Performance Evaluation of Type-H Inlets

An Abstract of
the

Thesis presented to

The faculty of Department of Civil and Environmental Engineering
University of Houston

In partial fulfillment
of the requirements for the degree

Master of Science

In

Civil Engineering

by:

Abhijeet Shreeram Bobde

December 2007

Abstract

Use of grate type in highway drainage is common on Texas Department of Transportation highways, but there is a lack of a formal, tested methodology for the design of these inlets. This research, funded by Texas Department of Transportation defines a basis for the design of H-inlets.

Literature reported experimental data for 3 different inlet morphologies was analyzed to determine the measured factors that predict the efficiency. An efficient inlet is the one which can drain maximum water; there are other competing requirements for the design of a good inlet such as safety, strength and debris handling. So far, efficiency of inlets was studied as a function of the flow volume and slope of the flow channel. In the present research, importance was given on use of non-dimensional variables and geometric ratios particular to the inlet to relate the hydraulic efficiency to these variables. The goal is to develop design methods generalized for inlets of similar morphologies independent of specific physical dimensions. The aim was to convert experimental data into non-dimensional charts to guide future experiments.

Chapter 1

Introduction

Type H Inlets are frequently used by the Texas Department of Transportation (Tx-DOT) as median drains for divided highways. Two varieties of Type H inlets are used, one of which is the Horizontal Inlet (Type H) with grate top and the other is the Horizontal Inlet (Type H) with lid. These are illustrated in TxDOT construction details IL-H-G and IL-HL. In spite of frequent use, engineers do not have adequate design information to mathematically describe the hydraulic performance of these structures.

Typically, it has been assumed that IL-H-G and IL-H-L function essentially the same as road-way grates or curb inlets, but there is no engineering basis for this assumption. Discussion of current limitations of design procedures is presented in Thompson et.al. (2004). However, the orientations in which the horizontal inlets can be used, deviate substantially from those of a roadway grate or curb inlets. Figure 1 is an image of a Type-H inlet near Jarrell, Texas. This particular inlet has vertical walls in the space between the grate longitudinal bars (horizontal in the image). In the context of "Traffic-Safe", this inlet is designed to prevent the wheel of a vehicle from entering the inlet; bicycle and pedestrian traffic (if the location were actually in such a place) would be impeded.

Figure 1. Representative Type-H Inlet (grate top) near I-35 at Jarrell, Texas.

Figure 2 is another Type-H inlet that looks nearly the same, except that the vault box is the size of the grate and the walls in the space between the grate and inlet are gently sloped to the vault. In the context of “Traffic-Safe", this inlet is also designed to prevent the wheel of a vehicle from entering the inlet; bicycle wheels might be excluded because the grate cross bar spacing is smaller than in the Jarrell, Texas inlet.

Figure 2. Type-H Inlet (grate top), sloped entry. I-35 feeder near San Marcos, Texas.

Figure 3. Grate-inlet (not Type-H) that is representative of the type of grate inlets that Type-H inlet (grate top) hydraulics is thought to mimic.

The objective of this research is to evaluate the hydraulic performance of the horizontal inlets, both grate-top and lid-top through non-dimensional analysis and produce results which can be synthesized into a series of algorithms for design purpose.

Figure 3 shows type of grate inlet with a lid top which is not type-H inlet but the hydraulics of this inlet are currently considered similar to that of a type-H inlet. Figure 4 shows a road side grate inlet which is not a type-H inlet but is commonly used as a median inlet.

Figure 4. Roadside grate inlet. I-35 feeder near San Marcos, Texas.

Chapter 2

Literature Review

2.1 Background and Scope of Literature Review

Inlet design for highway drainage is a complex problem because the designer needs to balance several competing objectives; high capacity for flow interception, operational safety, constructability and maintenance economy. The TxDOT Hydraulic Design Manual (2004), Chapter 10, Section 5, provides design guidance for several structures used for pavement drainage. These structures include curb inlets, grated inlets and slotted drains. Included in that chapter are necessary formulae and charts. Along with detailed charts, the Tx DOT Hydraulic Design Manual (2004), also include computation examples. The primary focus of this material is roadside drainage, primarily at the curb. Methods presented include use of combination inlets, inlets in sag configurations and carryover design approaches.

Sources for these approaches originate from selected reports by the National Cooperative Highway Research Program (Transportation Research Board, 1969), the American Association of State Highway and Transportation Officials (AASHTO, 1974), and the Federal Highway Administration (Johnson and Chang, 1987; Brown et. al., 2001; FHWA, 2001). Examples of design procedures appear in the Tx DOT manual and are similar to those of other states (e.g. Wisconsin DOT, (1997)) This literature review is focused on grated inlets, which are morphologically similar to the TxDOT Type-H inlet, especially their [grated

inlets] hydraulic performance in various situations. Additionally, the literature search paid attention to discovery of design guidelines with supporting experimental data as much to guide the physical modeling experiments as to understand the design principles applied elsewhere.

Most literature give importance to the hydraulic efficiency of inlet and safety for pedestrian and bicycle rides. Reports by St. Anthony Falls Laboratory Minnesota involved experiments to study the debris handling capacity of inlet (Larson, 1947; Larson, 1948)

A number of grate inlets have been experimentally examined in studies conducted by other state DOTs, and some federal facilities. Many of these experiments were full or nearly full-scale.

The main hydraulic focus in these studies was given on a grate being efficient and safe for the public. The purpose of many of these experiments was to identify an efficient grate inlet with a balance of the following qualities:

1. Hydraulic efficiency: The definition of the term "efficiency" varies slightly with different researchers, however here "efficiency" is referred to as the volume intercepted per unit volume of approach flow, approach flow is the total flow in the gutter flowing towards the inlet. Equation 1 represents this equation.

$$E = \frac{Q_{inlet}}{Q_{total}} \qquad (1)$$

where, Q_{total} is the total approach discharge, Q_{inlet} is the discharge intercepted by the inlet, and $Q_{co} = Q_{total} - Q_{inlet}$ is the carry-over discharge (discharge not intercepted by inlet). The definition of efficiency as presented is the flow fraction captured by the inlet; in some reports slightly other definitions were used; however there is sufficient documentation in each to use the flow fraction definition of Equation 1.

2. Safety in operation: Relatively recent work on inlet grates to accommodate bicycle and pedestrian use focuses on user safety. The principles involved will apply on type-H applications (except bicycle and pedestrian issues may be irrelevant for type-H use).

3. Strength

4. Stability: Again probably referring to bicycle use - stable means the grate is not easily dislodged during normal use.

5. Self Cleaning: Clogging in the literature was a motivation of several studies, despite the obvious loss of hydraulic capacity, clogging created other concerns in bicycle and other inlets. A handful of the reports mentioned some ad-hoc approaches to address clogging by cross member geometry, shape, and orientation. Simulated experiments using paper as a model for standard debris were performed.

6. Economics - both fabrication and maintenance.

2.2 Inlet Capacity Studies - Typical Experimental Design

The typical physical experimental design setup for quantification of grate inlet efficiencies is depicted in Figure 5. The typical configuration is a test channel

(flume) with the test grate in the bed to intercept the approach discharge. In most of the studies the longitudinal slope (slope in the flow direction) is adjustable.

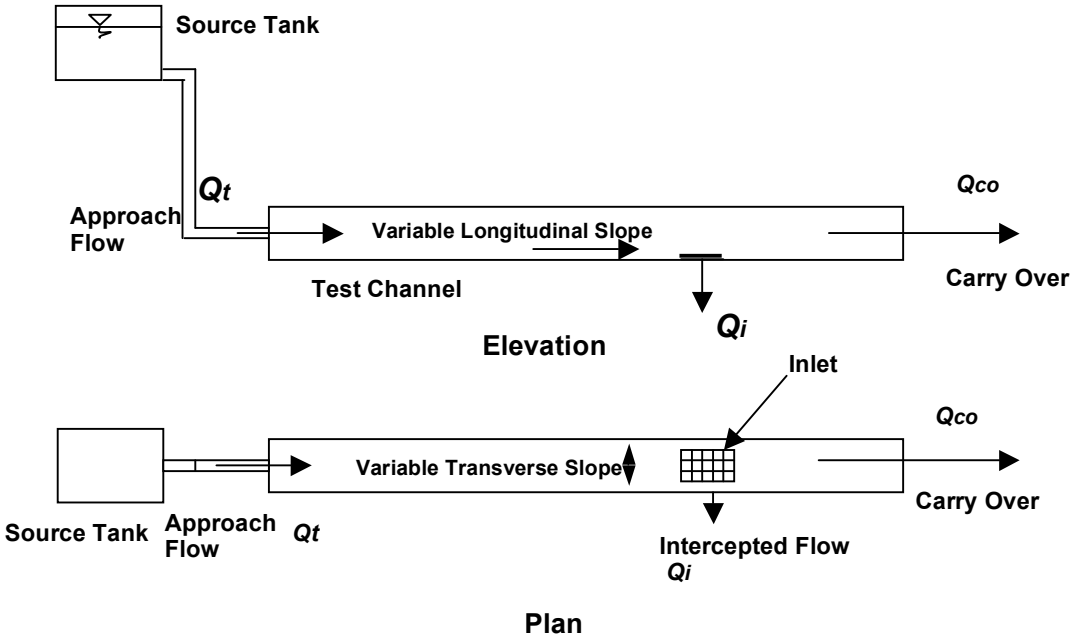

Figure 5. Typical physical modeling configuration.

In some experiments the transverse slope was also adjustable, aimed to incorporate the hydraulic effect of road crown. Lastly, some experiments included a curb-section, not being specific to in-grade inlets, grated curb inlets are a subset of grate inlets. Furthermore the data are deemed valuable as the curb does create an axis of symmetry and these data can be relevant for Type-H guidance. The inflow discharge, surface roughness and slopes in these channels are then

varied over a realistic range to observe hydraulic performance - the resulting measurements then form the database for inlet design computations.

As a minimum most of the reports studied collected and reported the following measurements in some form:

1. Total discharge.
2. Inlet discharge or hydraulic efficiency as defined above.
3. Longitudinal slope (dimensionless, percent slope, or feet-per-mile).
4. Transverse slope (dimensionless, percent slope, or feet-per-mile).
5. Width of spread: Width of spread is actually the flow expanse perpendicular to the direction of flow. This value is important in inlet design for maintaining serviceability of the roadway. If the spread width is too wide the roadway is flooded and is unsafe. Moreover, some literature related width of spread to the hydraulic efficiency of the inlet, the higher the width of spread, the lower will be the percentage interception (or efficiency). Different reports had different goals for what value was acceptable, but the concept is common to all studies.
6. Channel roughness or similar measure related to flow friction.

A variety of discharge measurement techniques were employed. For example the U.S. Bureau of Reclamation, (Woo and Jones, 1974) used a wooden flume 20 feet long and 35 feet wide to simulate a gutter. The longitudinal slope was varied using a mechanism for tilting the entire set up and transverse slope fixed at 0.04-dimensionless slope. Flow (approach flow) was measured using a venturi-meter at

the supply tank for small values and an annular flow meter for large values. Bypass (carryover) flow was measured by a weir. In addition to all these, point gages were employed to measure the water depth at the weir crest over the carryover collecting tank and another to measure the water depth in the flume. Approach flow was varied from 0.3 cfs to 3.2 cfs and longitudinal slope from 0.005 to 0.130. Roughness coefficient of the flume was varied by use of enamel paint on the inside surface of the wooden flume. Six different grates, each representative of a particular category were tested.

Flow measurement technology has changed since those experiments and modern techniques would likely use a combination of acoustic velocimetry and/or laser-Doppler velocimetry; however weir flows are simple backups to such tools. None of the reports studied appeared to use mass flow measurements (weigh water as it passes a section) although the laboratories involved had the capacity to make such measurements.

Table 1. Comparative experimental designs.

Organization	USBR	Florida DOT[1]	Minnesota DOT	Neenah Inc.[2]
Geo. Scale	1:1.27	1:2	1:1	1:1
Length (feet)	20	20	21	25
Width (feet)	3	--	3	4
Q_t (cfs)	0.003-3.2	--	--	--
Slope (Long.)	0.005-0.130	0.008-0.08	0-0.06	0.001-0.01
Material	Wood	PVC	Masonite	Concrete
Inlets Studied	6	3	9	--
Meas. Q_t	Venturi	--	Orifice ΔP	Orifice ΔP
Meas. Q_i	No	No	Yes	No

Notes: -- indicates a value is not available.
[1] Kranc and Anderson (1993); Kranc (2000)
[2] Neenah Foundry Co. (2007)

Table 1 compares the different selected experimental designs for which data are available. Of particular note is that the studies in the table all measure Q_{co} and compute Q_{inlet} from conservation of volume principles; a likely consequence of adapting existing flumes with overflow weirs to these kinds of experiments.

2.3 Debris Handling

Debris handling was an important theme in the Minnesota DOT (Larson, 1947) study. Figure 6 is an image of a grate inlet along a curb. The image is from a municipal street, but illustrates the debris issue as well as typical grate sizing.

The vehicle travel lanes are towards the top of the image. The image displays typical debris residue build-up after a drainage event, as well as a representative inlet opening size, about the size of a soda bottle as large as possible but small enough to exclude people's shoes. This study examined the response of grate inlets to debris under the assumption that dried leaves were the representative debris.

Figure 6. Image of Curb and Grate Inlet with Debris Residue.

The leaves themselves were simulated using reasonably sized papers. These numbered papers (a drift-tracer concept) were introduced in the approach flow after soaking them completely in water and then the number of paper pieces trapped, bypassed and intercepted was counted. Of particular significance these drift paper tracers probably represent a good surrogate for direct measurement of Q_{inlet}, and it is unfortunate that only summary results are presented for these drift tracer studies.

2.4 Findings of Prior Researchers

This section summarizes some of the findings reported in the reviewed studies. Some examples of how prior researchers presented their results are illustrated and synthesized in this section.

2.4.1 Inlet Capacity - Grate Inlets

The results in all reports were presented in a number of graphs and charts, wherein the inlet interception capacity has been plotted against each of the various factors which have an effect in the behavior of the inlets (longitudinal slope, approach flow quantity, cross slope and surface roughness of the inside of the test bed) while keeping the other factors constant for each test.

Figure 7 shows an example of a plot of hydraulic efficiencies against various values of approach flows for different grates. This chart is representative of the type of result presentations in all reports. The different curves on the chart are different grates. Notice the chart is dimensional - that is the discharge is in units of L^3T^{-1}.

The chart shows the anticipated response for the grates tested; specifically that the hydraulic efficiency (inlet flow fraction) decline with increase in the total flow. For lower values of total flow some of the inlets intercept 100%.

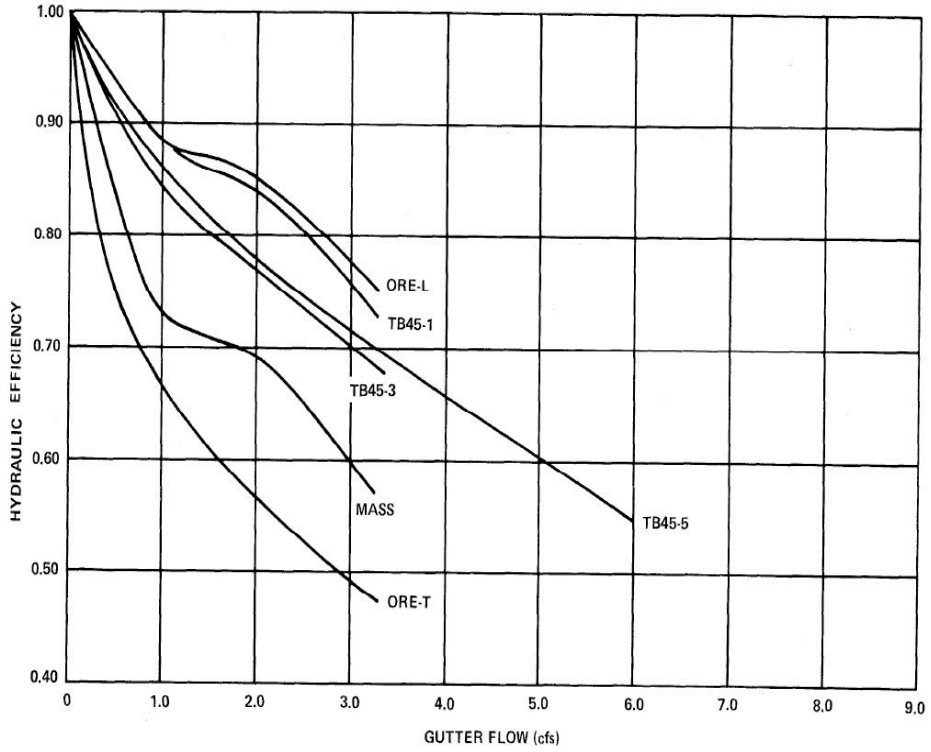

Figure7. Typical results presentation (Woo and Jones, 1974).

The Minnesota DOT (Larson, 1947) study noted that acceptance for a prescribed amount of carryover (deliberately by increasing total gutter flow and/or longitudinal slope) considerably increases the efficiency (flow fraction intercepted) of the inlet. This increase in interception is because the inlet head is increased (deeper submergence), and because of the way efficiency is defined (flow fraction). The report stated that a carryover allowance of 0.10 to 0.20 cubic feet per second increases the interception capacity by almost 100%. The

dimensional nature of the results makes comparison to other studies difficult. The observation advocating the deliberate allowance of carryover makes it more interesting to study how inlets in cascades would behave.

Findings of the experiments done by other researchers are summarized in the following list:

1. The inlet hydraulic capacity is affected by the characteristics of the inlet as well as the characteristics of the approach flow.
2. Variations in the approach flow produce different effects depending on the characteristics of the inlet.
3. The efficiency of a grate inlet to intercept all or a part of the gutter flow depends on the configuration and length of the grate as well as the longitudinal slope of the bed.
4. Any transverse elements (elements normal to the direction of flow) on a grate tend to cause the water to splash and skip over the grate thereby increasing the carryover and reducing efficiency.
5. Experiments to date are incapable of fully explaining the differences in behavior of different inlets from carryover that is bypassing the inlet by virtue of splashing as compared to carryover that is water simply flowing around the inlet. As a practical guideline, the interception width of the inlet is limited to the water flowing in the portion equal to the width of the grate.

Additionally, a study of inlets (Woo and Jones, 1974) with and without tilted transverse bars showed that effect of tilting the bars to provide a greater vertical opening on the upstream face, always increases the efficiency for all test conditions and further increases with increase in spacing of the transverse bars.

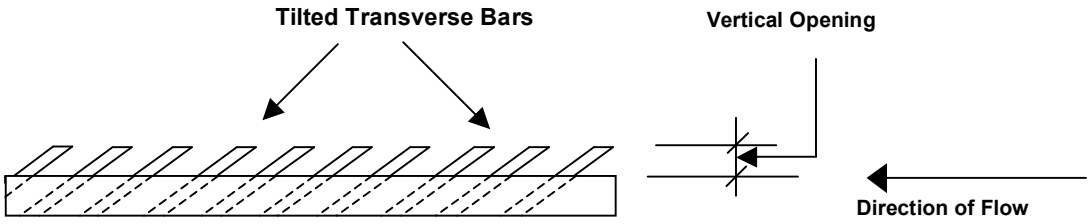

Figure 8. Schematic (profile view) of tilted-bar inlet. Each bar acts like a scoop. (Adapted from Woo and Jones, 1974).

Figure 8 shows the cross section of an inlet with tilted transverse bars. Although the transverse bars act like a scoop, this particular arrangement is also takes advantage of the Coanda effect, where the high speed flow will bend around an object if the approach angle is ideal. Figure 9 is an image of such a slanted-vane inlet in service. The image is serving as parking lot drainage in Richland, WA – while not in Texas; the image is representative of the specialized grate.

The prior research found that if widely spaced longitudinal bars are incorporated so as to maximize interception and transverse elements are avoided, the inlet

would be efficient but not safe for bicycle riders and pedestrians --- an open hole being the most efficient design in this context.

Figure 9. Slanted-vane type grate inlet.

Conversely, closely spaced longitudinal bars and transverse bars would be safe, but severely restrict the interception of incoming flow; in the limit behaving as a porous medium with negligible interception in the context and time frame of highway drainage for which inlets are currently used.

Larson, (1947) determined that rounded bars as grate elements increases the effective length of openings in the grates. For example, for a given length and width of an inlet, if rounded bars are used instead of square bars the area of openings are slightly increased with proportionate interception capacity increase. The mechanics of this increase is a manifestation of the Coanda-effect caused by the circular path presented by the bar cross section. In liquid systems this effect is usually quite small, and Larson's observations are of some significance from a

scientific standpoint, however rectangular bars are easier to fabricate and are likely to remain the geometry of choice.

Kranc, (2000) observed that the inlet performance depends primarily on the upstream depth and less on other factors like bed slope or velocity. His experiments also observed that lowest slope is not the most efficient slope, because at low velocities on flat slope transverse spread is considerably greater and the inlet is not able to intercept all of the flow. Although higher velocities of approach flow tend to cause splashing over the grates and reduce interception --- thus favoring a reduction in slope if possible, there is also a simultaneous increase in interception of flow because more water is concentrated in the area covered by the width of the inlet. His experiments also reported that forced ponding near the inlet by introducing a barrier downstream of inlet can increase interception by about 35%.

2.5 Debris Handling – Grate Inlets

Debris handling experiments (Larson, 1947) focused on the hydraulic capacity while debris is entrained in the water. Generally, the experiments observed that the inlets with wider spacing and bars parallel to the flow direction are more efficient (to the order of 95%) in intercepting and passing flows containing debris. For other grates it was observed that once the debris pieces are trapped in the upstream part of the inlet the frictional pull due to the water flowing over it may drag and carry off the debris. Specially baffled bars were designed to minimize

trapping of debris particles; however these inlets could not deliver satisfactory hydraulic performance. The study was further discontinued.

2.6 Inlet Capacity - Curb and Gutter Inlets

This subsection examines the literature related to curb inlets. Type-H inlets with lid tops are anticipated to behave closer to curb-type inlet than to grate-type inlets; hence the experimental design is expected to be similar.

McEnroe and others (1999) studied four standard deigns for curb and gutter inlets, the concrete gutter inlet, a curb inlet and a combination inlet. The hydraulic model studies of these inlets were carried out in the University of Kansas on a one-quarter scale using a simulated roadway with variable longitudinal and cross slope. The test roadway is 15 m long and set up with weir for discharge measurement. There is also a V-notch weir which is calibrated using a head discharge relationship. Tests were carried out with longitudinal slopes of 0.5%, 1%, 2%, 3% and 5% and cross slopes of 1.6%. The objective was to determine the relationships between the captured and total discharge.

The researchers reported that relationship between captured discharge and total discharge for each set-up can be represented by design curves that relate different inlets to performance. In some cases these design curve apply to all the grades and in some cases a separate design curve applies. They also observed that the grade has little effect on the inlets. The performance of some inlets is marginally better

on steep grades (up to 5%) than on mild grades (around 0.5%) and its opposite for other inlets. All of the inlets perform better on steeper cross slopes. One particular inlet (Type B in their study) was identified as a design that performed the same (constant efficiency) irrespective of the test conditions.

2.7 Design Methods

This section reviews general design methods used in inlet design and selection.

2.7.1 General Approach

Inlet design methods generally require an estimation of discharge that is expected, and specification of acceptable spread (pond width in the highway). A factor of safety for these values is suggested (ASCE, 1993) at this point, after which the inlet hydraulics are specified and ultimately the inlets sized and placed. The sizing is usually based on charts contained in various design guidelines, and on empirical (regression) equations that use existing slopes, physical characteristics of grades and pavements, and spacing of inlets as explanatory variables to predict performance of the inlet.

Spacing of successive inlets on a grade is one explanatory factor for which little experimental data exist. So far no experimental studies have been found which analyze cascaded inlets and their collective behavior. The effect of cascades is beyond the scope of the current project, but is acknowledged as the next important area of experimentation. Numerical modeling using computational fluid

dynamics (CFD) techniques may be adequate to explain collective behavior and field monitoring to verify modeling results sufficiently.

Chapter 3

Problem Statement

Currently design of H-inlets used in highway medians is somewhat arbitrary and based on comparison with other intake structures; there is no engineering basis for this comparison. Under these conditions the use of H-inlets might not be the best possible in terms of performance, some inlets might be underperforming and some might never be required to use their capacities. In a broader sense the aim of this research is to build an engineering base for the design of H-inlets, so that in future, inlets designed would perform better in terms of their capacities to drain water and with optimum use of resources.

Because of too many competing requirements of a "good" inlet, the analytical approach fails to understand the behavior of the inlet. Experimental data have been used to relate the behavior of the inlet to what are called as explanatory variables. These experiments were made to simulate the field performance of an inlet as closely as possible by selection of proper roughness of the channel, realistic slopes and flow discharges.

Wider ranges of variable were considered when The Bureau of Reclamation Denver, Colorado conducted the flow channel simulation experiments for determination of inlet efficiency for Federal Highway Administration (Burgi, 1978). The variables covered realistic ranges of longitudinal slope, flow volume, size of inlet (width and length), type of grate and spread width.

One important need of this research was to establish methods to construct mathematical relationships between the hydraulic efficiency of the inlet and the explanatory variables which could be used for general design of inlets. For this reason, non-dimensional variables were identified so that efficiency of an inlet can be expressed as a function of non-dimensional variables which makes it extendable for other designs. However different types of inlet vary in the shapes and orientation of their grates and because orientation of grates play an important role in the interception capacity of an inlet, then, in principle, it would be difficult to develop a unique mathematical relation between the variables and efficiency. The following chapter summarizes the procedure of "quantifying" different shapes and configurations of inlets to develop non-dimensional explanatory variables along with other variables which collectively form a correlation to define the inlet efficiency.

Chapter 4

Approach

4.1 Methods: Non-Dimensionalization of literature reported experimental data

Researchers at Saint Anthony Falls Laboratory, Minnesota, Florida DOT, Bureau of Reclamation, Denver, CO (for Federal Highway Administration) and Kansas DOT, performed experiments for studying behavior of different types of inlets. The experiments did not cover a wider variety of inlet types because the types included were mainly those of interest to the sponsor. However data for 3 main morphologies of inlets are available for study (Burgi, 1978b) which includes parallel bar inlet with no cross bar, parallel bar inlet with cross bars and curved vane type of inlet. This chapter details the data analysis of the available results of the above mentioned experiments and their modification into non-dimensional explanatory variables. Selection of Bureau of Reclamation, Denver, Co (for Federal Highway Administration, Burgi 1978b) data for analysis was owing to the size of data available in this report. The models are developed using this data and are validated using the data available in FL- DOT report (Woo and Jones, 1974).

Typical data available are in the form of plots of hydraulic efficiencies of inlets tested against various flow volumes (typical result graphs are shown in Chapter 2, Fig. 7). Hydraulic efficiency was calculated as the ratio of flow volume intercepted by the inlet to the volume of total approach flow. These efficiencies would be referred to as observed efficiencies hereafter. The result graphs have

different curves, each of which represent various longitudinal slopes of the flow channel. The different inlet types for which the data were available differed in area (different widths and lengths), presence or absence and shape of cross bars, spacing between cross bars, section of bars and structure of the cross bar (if present). Each inlet type was tested for slopes of 0.5%, 1%, 2%, 4%, 6%, 9% and 13%.

4.2 Inlet Morphologies

Reviewed literature (Burgi, 1978 b) has data sets for three different types of inlets, these inlets varied in the types of cross bars, spacing of bars and size of bars. These types are described in brief below:

P 1-1/8: Parallel longitudinal bars with no cross members and the spacing between adjacent parallel bars is 1 1/8 inch center to center and width of each bar is ¾ inch.

P 1- 7/8: Parallel longitudinal bars with cross members spaced 4 inch apart center to center, spacing between adjacent parallel bars is 1 7/8 inches center to center and width of each bar is ¼ inch.

CV 3- ¼: Longitudinal bars are placed 3 ¼ inch center to center and curved vane bearings are 4 ¼ inch center to center.

The above inlet types are sketched in detail in appendix A.

4.3 Identification of Non-Dimensional Variables:

The aim of the data analysis is to select variables which can be used to develop statistical models for inlets efficiency. Such variables can be compared, used for design purposes and extended for generalized design of inlets if they are non-dimensional. For a given inlet, the existing experimental results show efficiency as a function of channel slope and total approach flow. Comparison and extension of these graphical results for design purpose is not possible due to dimensional nature of the data. Analyzing the available data we come up with following five non-dimensional variables which would be used to relate to efficiency of inlet:

1.) Longitudinal Aspect Ratio (ratio of inlet width of to length , Figure 10)

2.) Effective Area Ratio (ratio of area of openings of inlet to its total area)

3.) Longitudinal Slope of Channel (Figure 17)

4.) Flow width ratio (figure 18)

5.) Froude Number

Each of these variables is been discussed in the next sections.

4.3.1 Longitudinal Aspect Ratio

Burgi (1978 b) observed that the wider the inlet, the more efficient it tends to be, as it is the width of the inlet though which most of the inflowing water is intercepted and if the flow volume is low, the flow may not even cross the whole length of the inlet. In Burgi's reference and in this discussion, the dimension of the inlet perpendicular to the direction of flow is taken as the width of the inlet while the other dimension parallel to the direction of flow is considered as the length of the inlet. Fig. 10 illustrates the selection of dimension with respect to the flow direction. Burgi further observed that widths of inlets have greater effect on

flow interception because for relatively narrower inlets water flowing through the channel may simply bypass the inlet by flowing over the side of the inlet. Having observed and established the importance of inlet width, if the model under development was to be extended for general design purposes, width could not be used as a variable for modeling. The reason was its dimensional nature.

Ratio of width of inlet to its length is defined as the longitudinal aspect ratio of the inlet. This definition holds well with a lone criterion of placement of the inlet with respect to the flow direction and irrespective of the configuration of grates which it may have.

The non-dimensional variable of longitudinal aspect ratio $\frac{W}{L}$ is proposed as a key variable which may have an effect on the efficiency of the inlet or in other words an inlet characteristic which can be used in conjunction with other variables to model the hydraulic efficiency of the inlet.

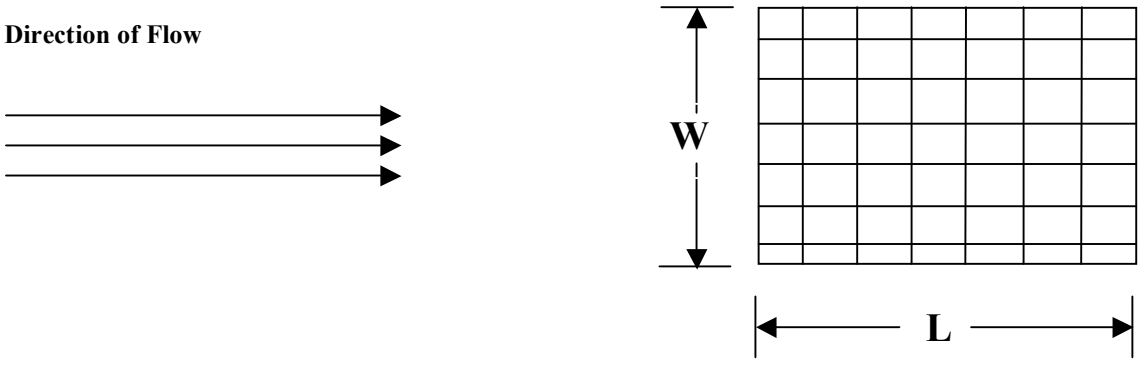

Figure 10. Dimensions of the inlet with respect to the direction of flow.

Cassidy (1966) expressed hydraulic efficiency of inlet in terms non-dimensional variables. Efficiency was expressed as a function of $\frac{V_o}{\sqrt{gD}}, \frac{D}{W}, \frac{L}{D}$ and slope,

where

V_o is Approach Velocity

D is Depth of Flow

W is Width of Inlet; and

L is Length of Inlet

However the experiments were limited to a single size of inlets (1 foot x 1 foot). The non-dimensional relations developed were useful in comparing absolute characteristics of two inlets.

Figure 11 is an example of typical results presentation. The figure present efficiencies for different flow conditions in form of charts with various longitudinal slopes, gutter flows, flow widths and sizes of inlets. These charts were converted into numerical data and tabulated as a requirement for computing values of the explanatory variables.

Table 2 (Burgi, 1978 b) shows the dimensions of different inlets and corresponding longitudinal aspect ratios for which the values of efficiencies at different flow volumes and slopes are available. For total flow volumes of 1, 2, 3, 4 and 5 CFS all values of efficiencies were plotted against longitudinal aspect ratios of the inlets.

Table 2. Dimensions and corresponding longitudinal aspect ratios of inlets *.

Width (feet)	Length (feet)	Longitudinal Aspect Ratio	Area (sq. ft)	No. of inlets tested
3	4	0.75	12	3
3	2	1.5	6	3
1.25	2.67	0.47	3.33	3
1.25	2	0.63	2.5	3

(* - Adapted from Burgi, 1978)

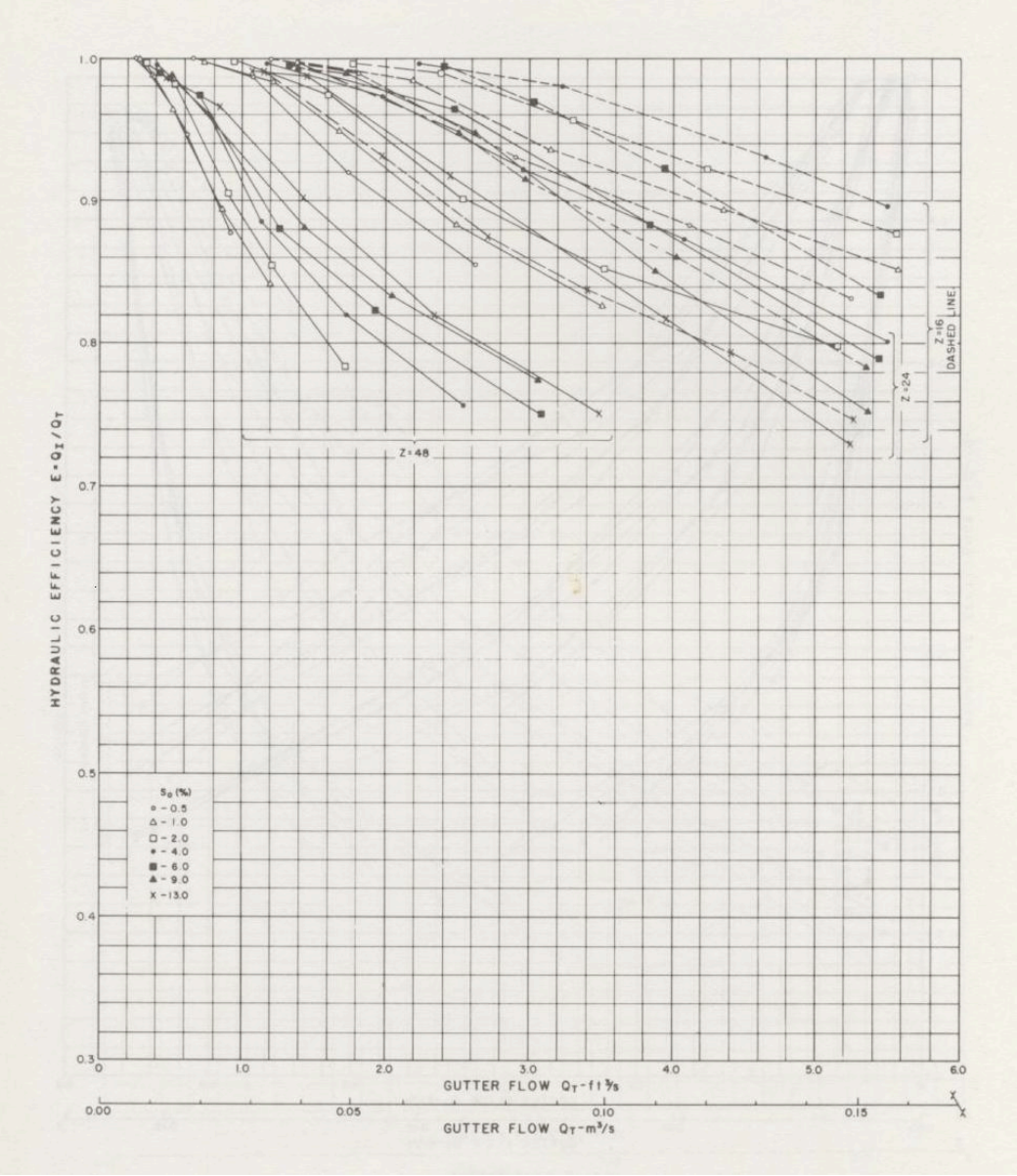

Figure 11. Typical result graphs which were converted into numerical data.

Figure 12 shows the graph of efficiency against longitudinal aspect ratios for P-1-1/8 inlet. It can be seen that longitudinal aspect ratio of 0.75 gives the maximum hydraulic efficiency. Figure 13 shows the plot of longitudinal aspect ratio for P 1-7/8 inlet and figure 14 shows the similar graph (longitudinal aspect ratio versus efficiency) for CV 3-1/4 inlet. All the graphs show that maximum efficiency

occurs at the W/L value of 0.75. The reason is made clear by the area of the inlet associated with the longitudinal aspect ratio of 0.75, 12 sq. feet which is much higher than all other inlets used.

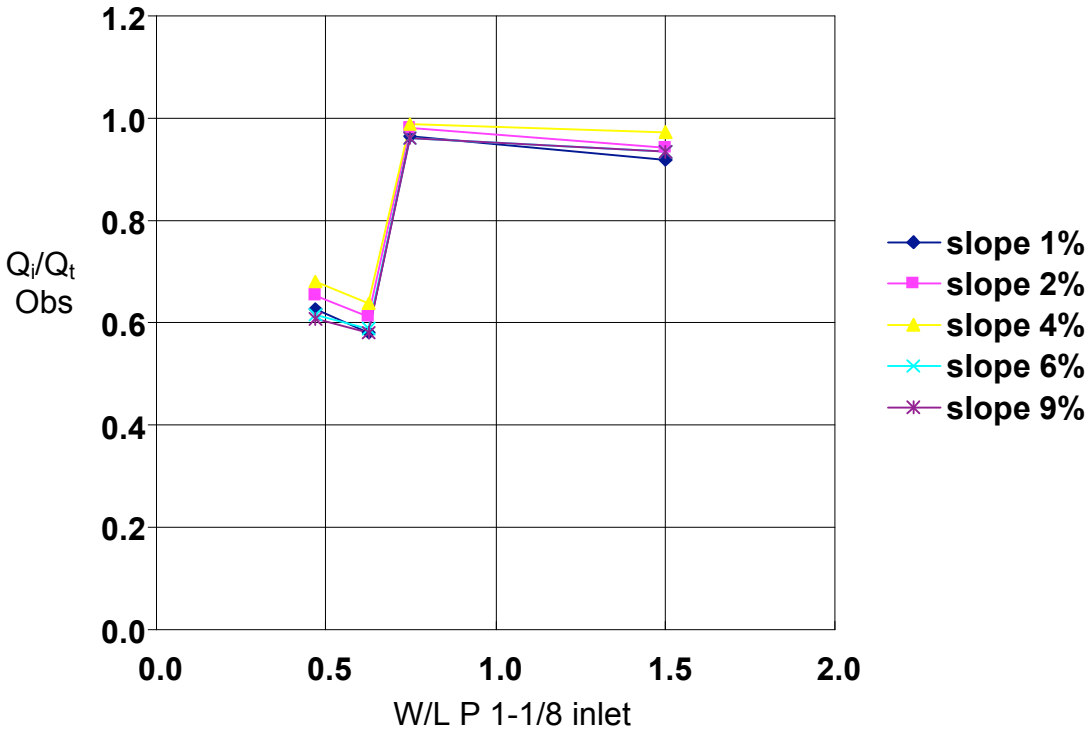

Figure 12. Efficiency vs longitudinal aspect ratio for inlet P 1-1/8.

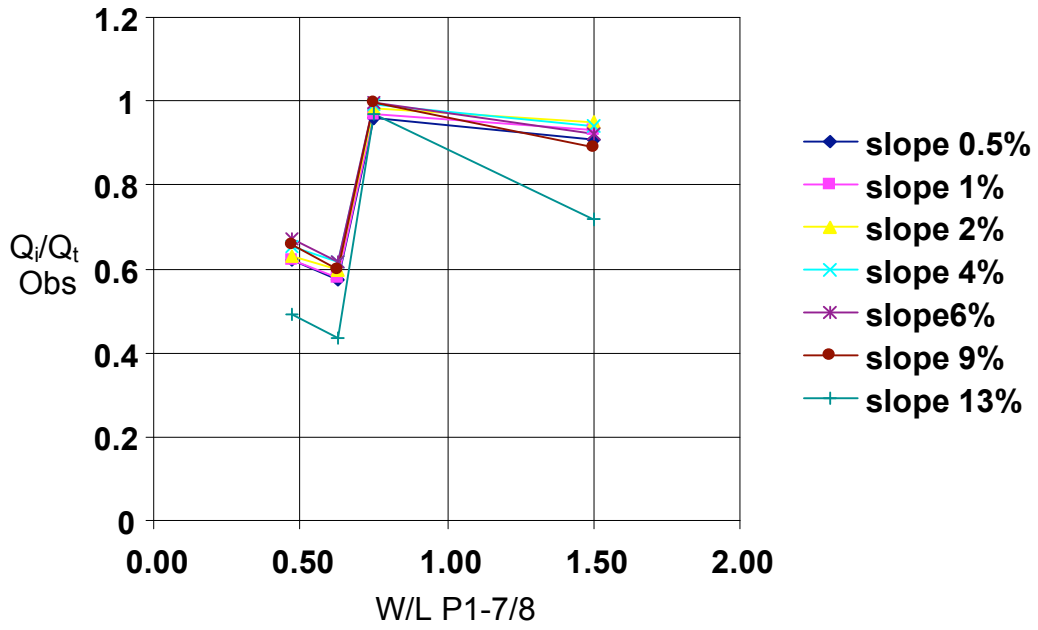

Figure 13. Efficiency vs longitudinal aspect ratio for inlet P 1-7/8.

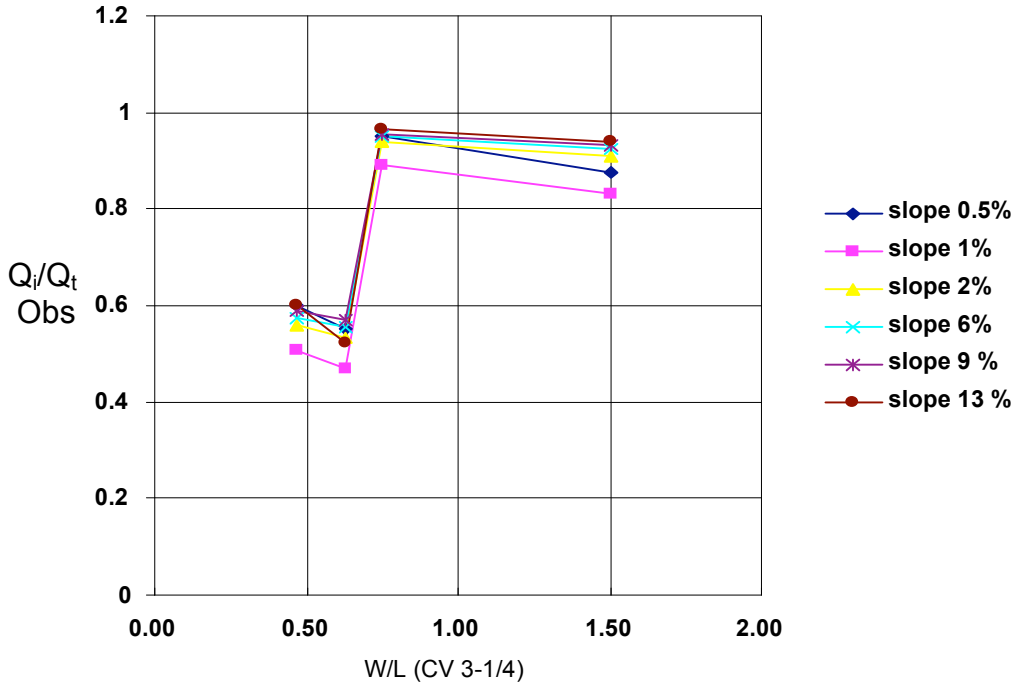

Figure 14. Efficiency vs longitudinal aspect ratio for inlet CV 3-1/4.

4.3.2 Effective area ratio (a_e):

Longitudinal aspect ratio alone cannot be used to define the efficiency of inlets. Area plays an important role too, a non-dimensional variable was needed which takes into account the area of the inlet. If hydraulic efficiency was the only objective of the design then an open hole would have been the best inlet, however for practical purposes an inlet has to be safe hence an open hole cannot be used. The area concept has the idea of using effective area of inlet as one of the key variables controlling the efficiency.

Again, area being a dimensional variable cannot be used as an extendable design parameter; hence the ratio of total area of opening in an inlet to the total area of inlet is proposed as a prospective explanatory variable.

The *'effective area ratio'* of an inlet is defined as the ratio of total area of openings of an inlet to its gross area.

Effective area ratio

$$a_e = \frac{a_o}{a_i}$$

Where,

a_o = Cumulative area of openings in the inlet

a_i = Gross area of the inlet

Figure 15 show the efficiency variation for P 1-1/8 inlet with different effective area ratios. A similar graph showing efficiencies for different effective area ratios for the P 1-7/8 inlet is shown in figure 16.

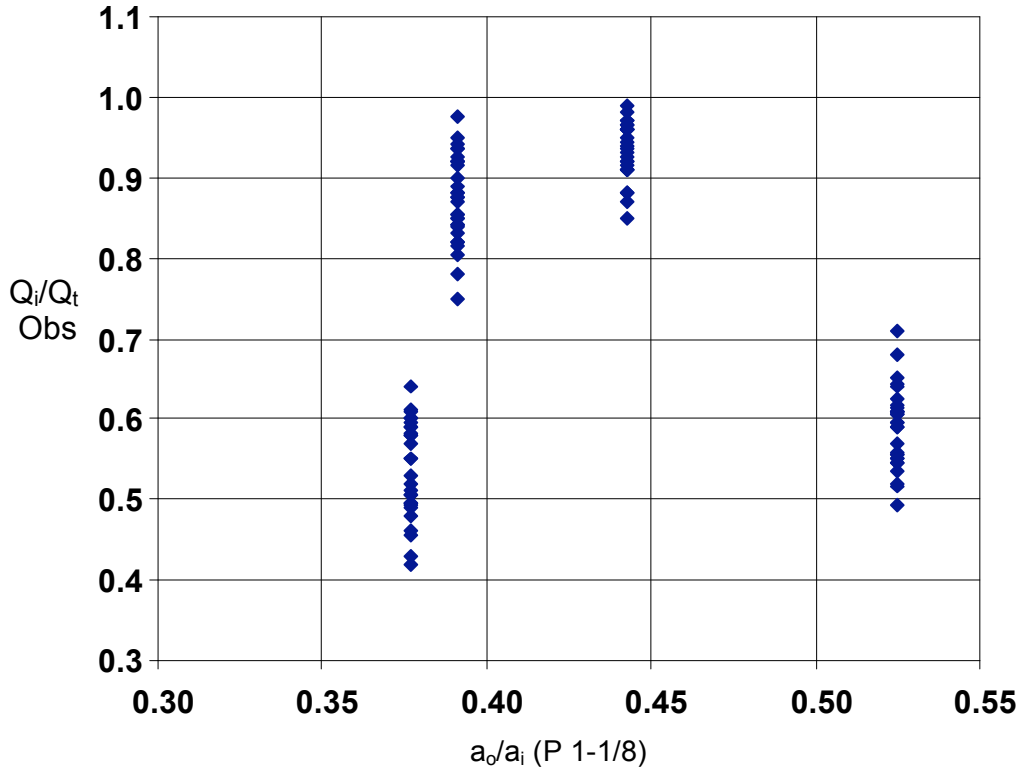

Figure 15. Efficiency values for different values of effective area ratio of inlet P 1-1/8.

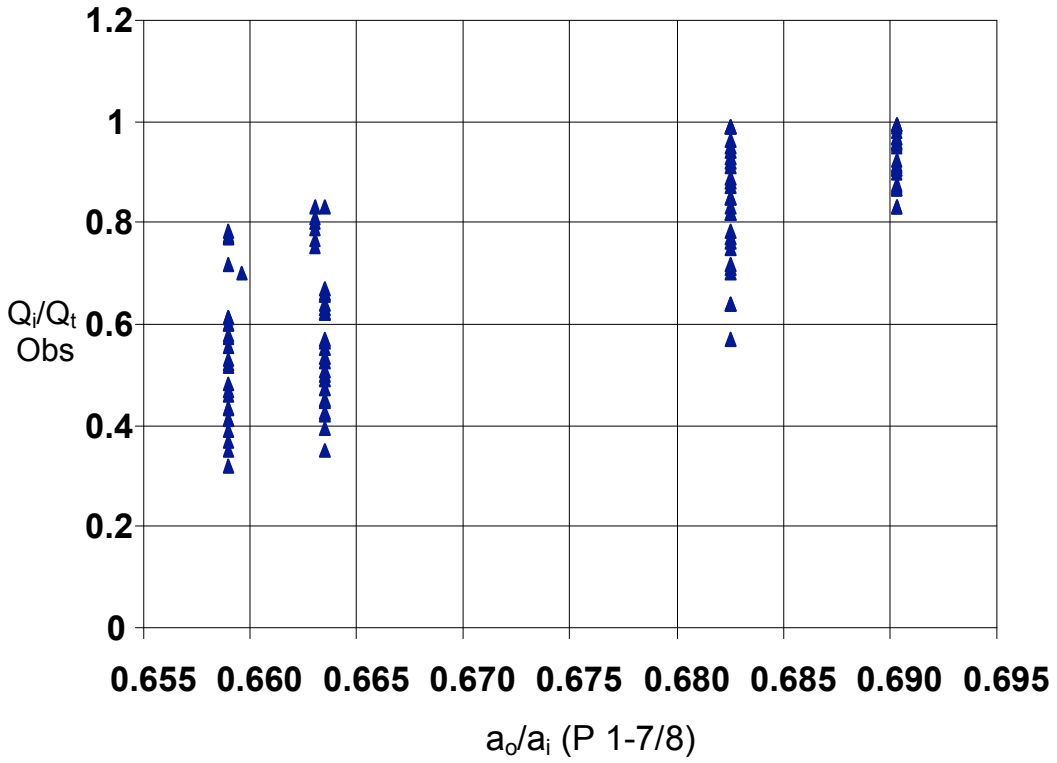

Figure 16. Efficiency values for different values of effective area ratio of inlet P 1-7/8.

Figure 17 show the efficiency variation for CV 3-1/4 inlet with different effective area ratios.

The interception capacity of an inlet depends on its (inlet's) interaction with the incoming flow. The physical characteristics of the inlet influence this interaction. Since the water enters the inlet through the openings, the effective area ratio is a logical variable which can be used as an explanatory variable.

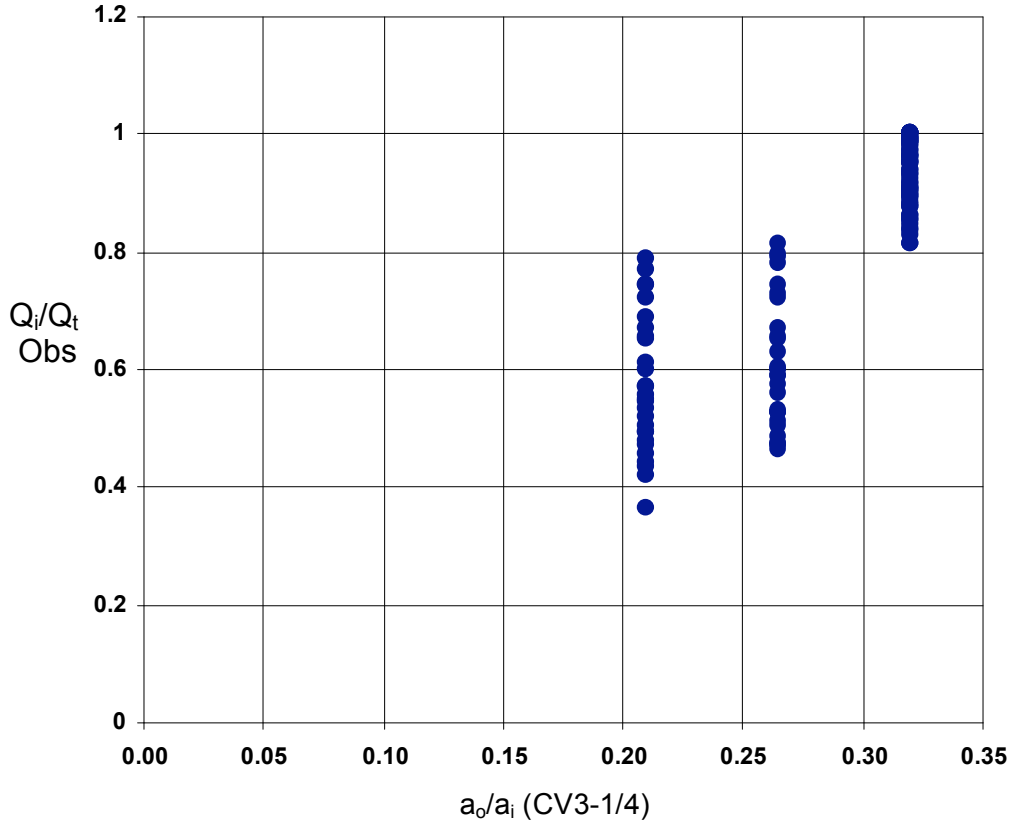

Figure 17. Efficiency values for different values of effective area ratio of inlet CV 3-1/4.

When used in conjunction with other non-dimensional variables effective area ratio may prove to be a key variable in developing a statistical model which can be extended for other types and sizes of inlets and can give a better understanding of the effect of inlet structure on its interception capacity. It should be noted that in each of the graphs shown in figures 15, 16 and 17, the axes showing the effective area ratio are on different scale.

4.3.3 Longitudinal Slope:

Most of the results reported in the literature studied report efficiency curves for different longitudinal slopes of the flow channel. Figure 18 (Burgi, 1978 b) shows one of these results where efficiency is plotted against total channel flow and different curves, each corresponding to a particular value of longitudinal slope of the flow channel clearly shows the effect of longitudinal slope on the hydraulic efficiency of the inlet. At steeper slopes inlets tend to be less efficient due to higher velocity of flowing water causing water to cross the inlet without sufficient time for interception and also causing splash over the cross members of the inlets. Higher velocities and splashing cause reduction in interception by the inlet but this reduction can be counteracted by the area of the inlet and the spread of the flow approaching the inlet. Hence slope of the flow channel cannot be the sole variable which controls the interception capacity of the inlet. Longitudinal slope of the flow channel is one of the key variables (non-dimensional) which will be used in modeling the efficiency of the inlet.

4.3.4 Flow Width Ratio:

Flow width ratio is defined as the ratio of width of flow to the width of the inlet. This particular ratio comes into picture when it is observed that even for low flow volumes at gentler slopes only that part of the inflow is intercepted by the inlet which physically crosses the inlet. Even for the most efficient inlet, some part of the water may simply bypass the inlet by flowing over the sides which would make the inlet relatively in-efficient in practical purposes.

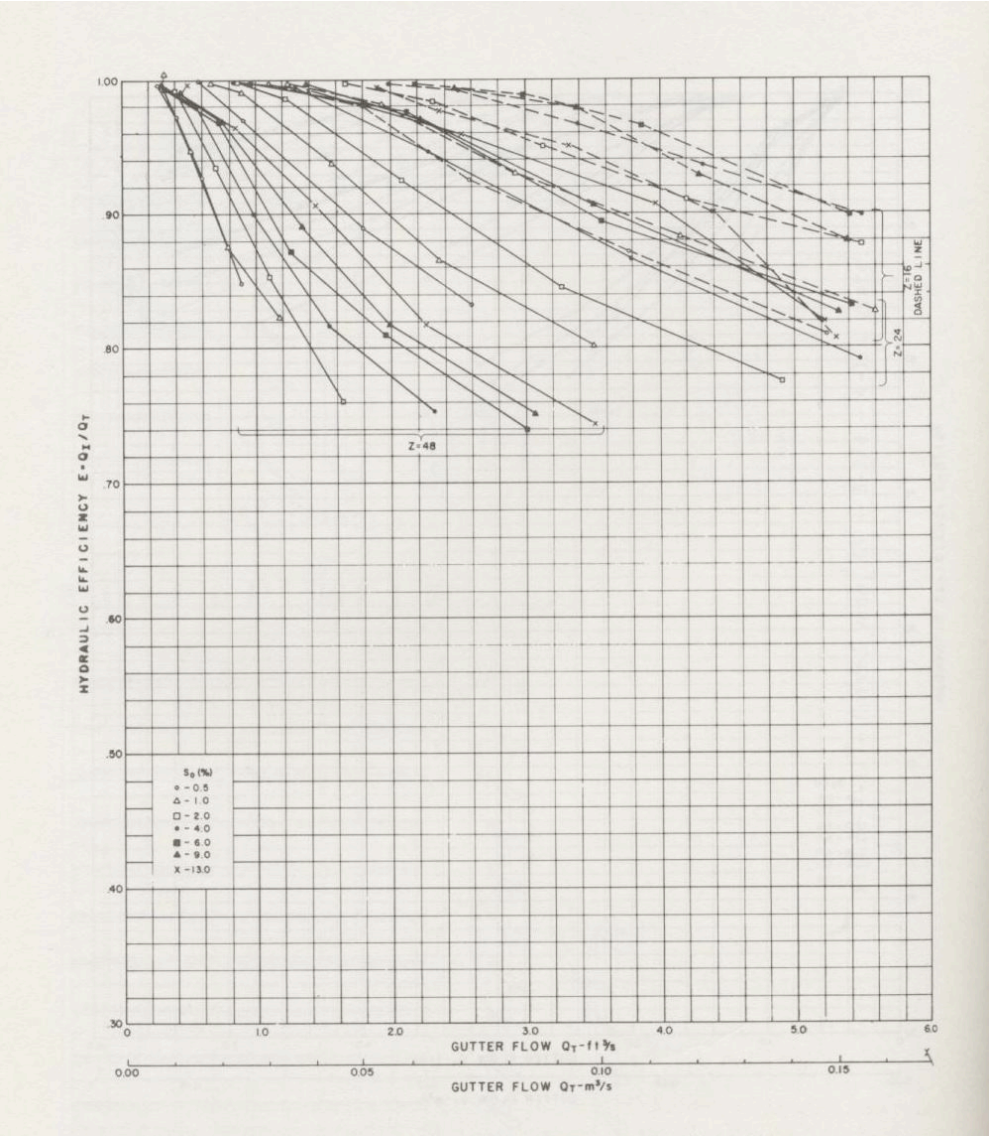

Figure 18. Image of typical result graphs of inlet efficiency plotted against total gutter flow at different slopes from the studied literature (Burgi, 1978).

Figure 19 shows the concept of relation between width of flow and width of inlet and the interception capacity of the inlet. For a given flow volume, the geometry of the flow channel (most importantly the cross slope of the channel) controls the width of incoming flow, hence an optimum width of inlet (depending of the flow width corresponding to the most probable flow volume) would ensure maximum

hydraulic efficiency. The *flow width ratio* is selected as the fourth explanatory variable that will be used to establish a model for hydraulic efficiency of the inlet.

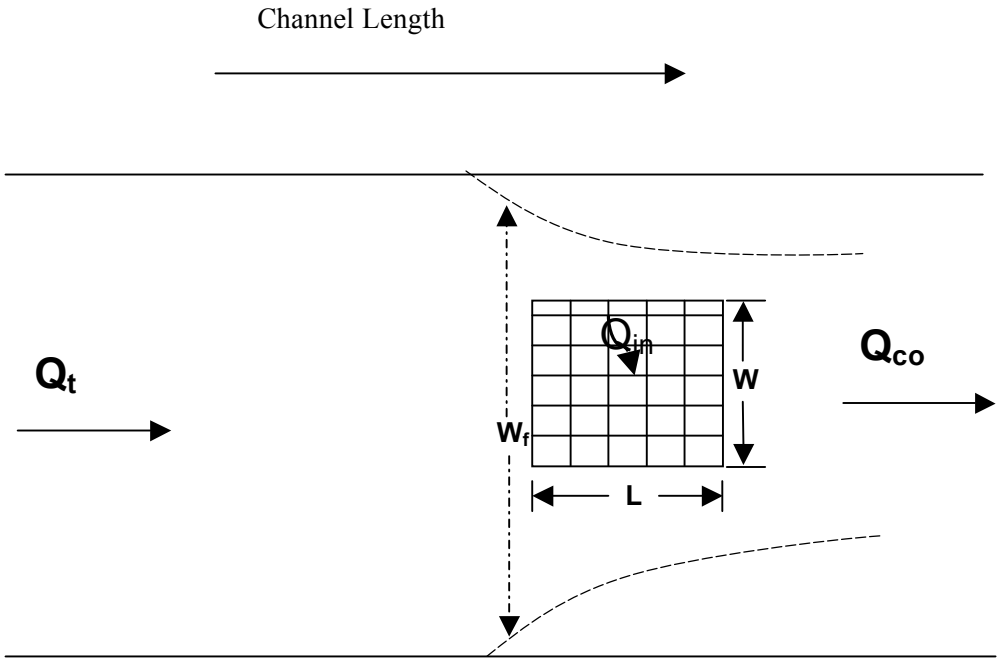

Flow width ratio = W/W_f

Figure 19. Width of flow and the inlet dimensions demonstrating the concept of flow width ratio.

4.3.5 Froude Number:

Cassidy (1966) made use of non-dimensional variables to express the efficiency of inlets. One of the non-dimensional variable used by Cassidy was $\frac{V_o}{\sqrt{gD}}$ (where V_o is velocity of approach flow and D is depth flow) which is a Froude number of the approaching flow. Velocity of flow has an effect on the interception by the inlet as does the flow depth, the use of a Froude number is therefore a logical

explanatory variable. However in the experiments conducted by Cassidy constant sizes of inlets were used (1 foot x 1foot) and no inlets with cross bars were tested.

Cross bars in an inlet cause splashing of the flow which tends to reduce the efficiency of the inlet and the reduction is more pronounced at higher velocities, thus velocity of flow becomes an important factor when it comes to interception, it is the interaction between the inlet and the flow which has an effect on the inlet efficiency. In Cassidy's study, inlet behavior for steeper longitudinal slopes was not studied, however the model proposed in this thesis takes in to account the flow velocity along with a wider range of longitudinal slopes. In the proposed model inlet efficiency is expressed as a function of longitudinal slope, effective area ratio, longitudinal aspect ratio and Froude number. The flow width is taken into consideration in the calculation of Froude number (Equation 2) hence the use of flow width ratio as a separate variable is neglected. Froude number was taken as

$$Froude\ Number = \frac{Flow\ Velocity}{Surface\ wave\ Speed}$$

$$Fr = \frac{V_0}{\sqrt{gD}}$$

$$Fr = \frac{Q}{W_f \sqrt{gD^3}} \tag{2}$$

where,

Q = Approach flow discharge (Q_t)

W_f= Width of flow

g = Acceleration due to gravity (32.17 fps^2)

D = Depth of flow at the centroid of the triangle of flow cross section

Figure 20 is a plot of the relationship between Froude number and P 1-1/8 inlet efficiency. The graph illustrates that with increase in Froude number the efficiency decreases. The solid line shown on the graph represents a trend line showing the inverse relationship between the Froude number and inlet efficiency. Figure 21 shows a similar plot for P 1-7/8 inlet in which the trend line on the graph shows an inverse relationship between Froude number and efficiency. It could be observed that the trend line on the P 1-1/8 inlet graph is flatter compared to that on P 1-7/8 inlet graph. Absence of a cross member (which causes splashing at higher velocities) in P 1-1/8 inlet could be the reason that with increase in approach velocity the efficiency decreases gently. Figure 22 shows the plot of Froude number and efficiency for the CV 3-1/4 inlet. Again the trend line shows an inverse relationship between Froude number and inlet efficiency. The trend line in the graph shown in figure 22 is flatter than that shown in figure 21 (P 1-7/8 inlet) inspite of the presence of cross members. The flatter trend line is because the cross members are curved vanes which extend above the plane of the inlet and aid in intercepting more inflow.

After identification of non-dimensional variables, the next step was to define a mathematical relationship which would relate these variables to the efficiency of the inlet and thereby make it a model which, on account of the non-dimensional

nature of the variables involved, will presumably be extendable to generalized design procedures.

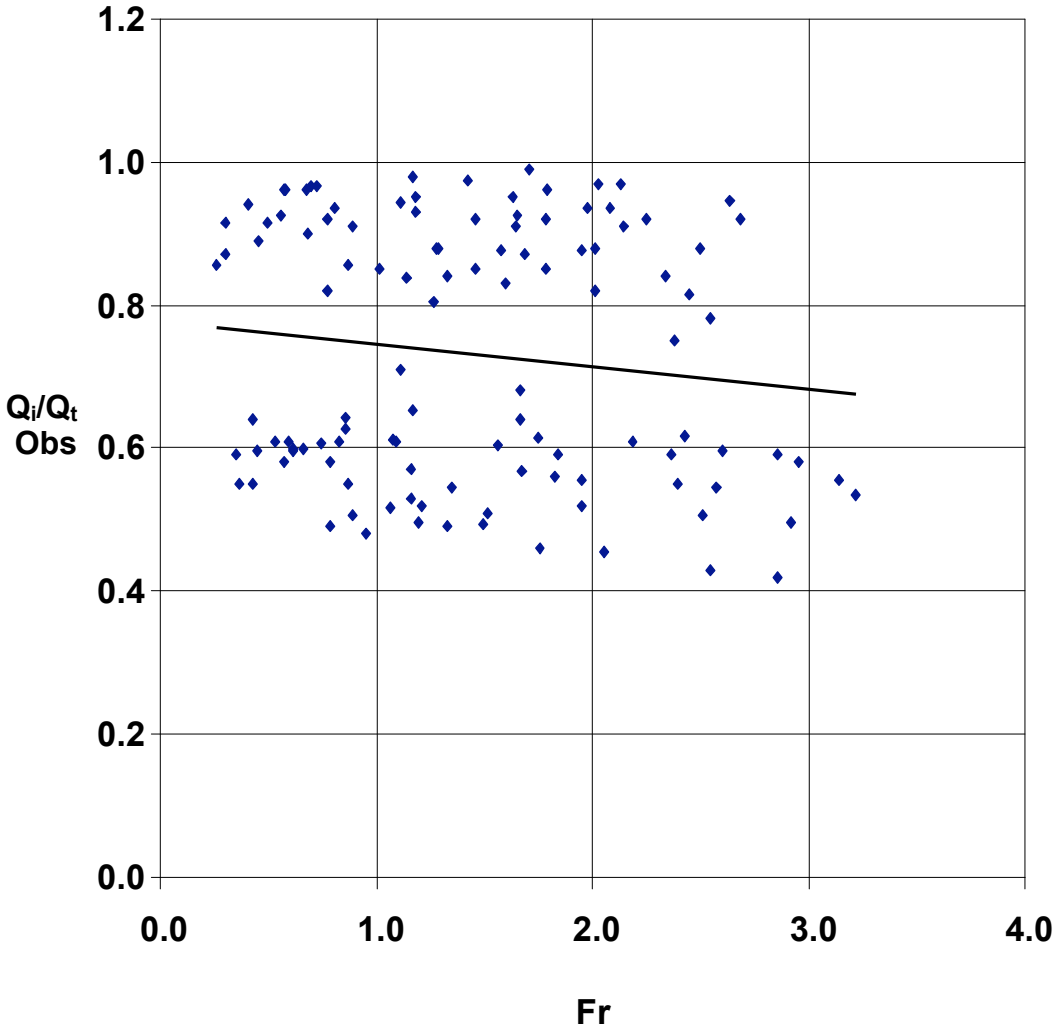

Figure 20. Plot of observed efficiency values and Froude number with a linear trend line (inlet P 1-1/8).

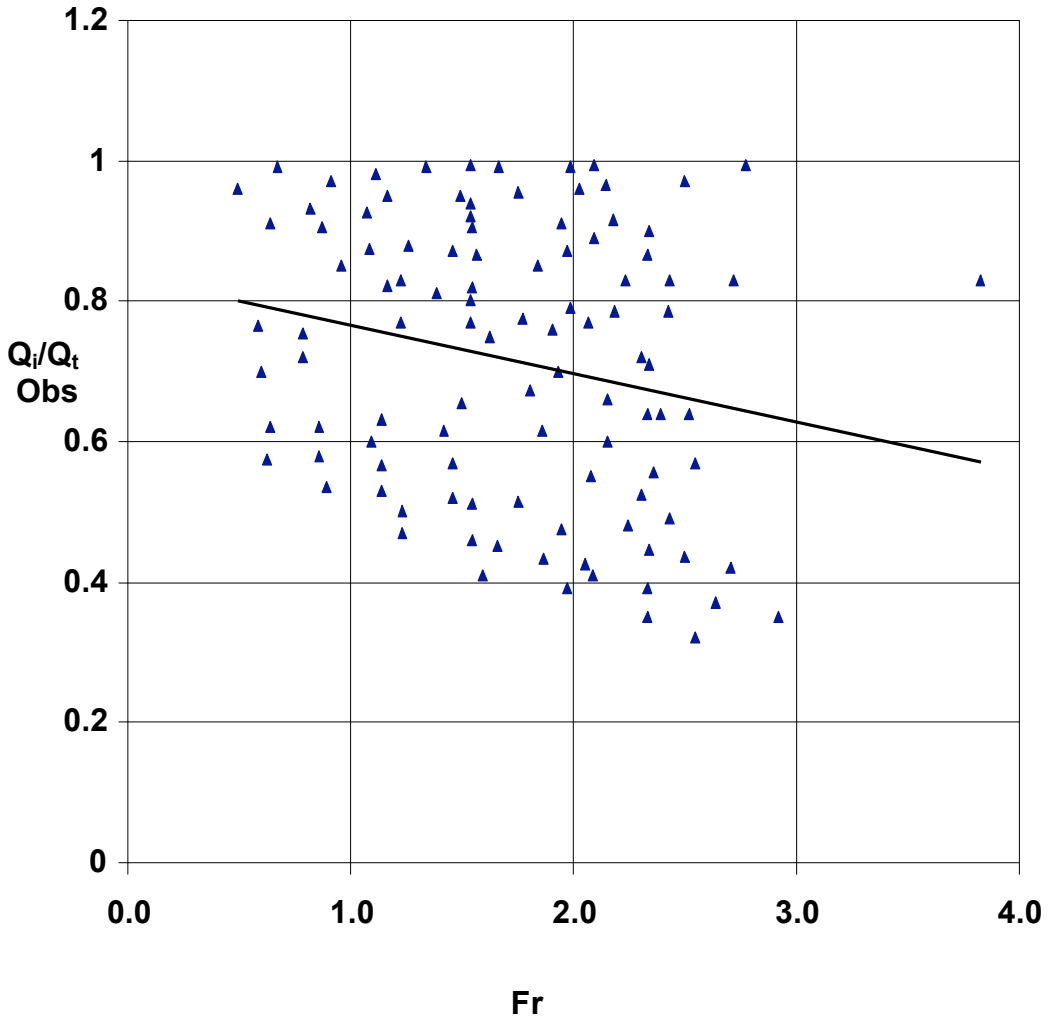

Figure 21. Plot of observed efficiency and Froude number with a linear trend line (P 1-7/8).

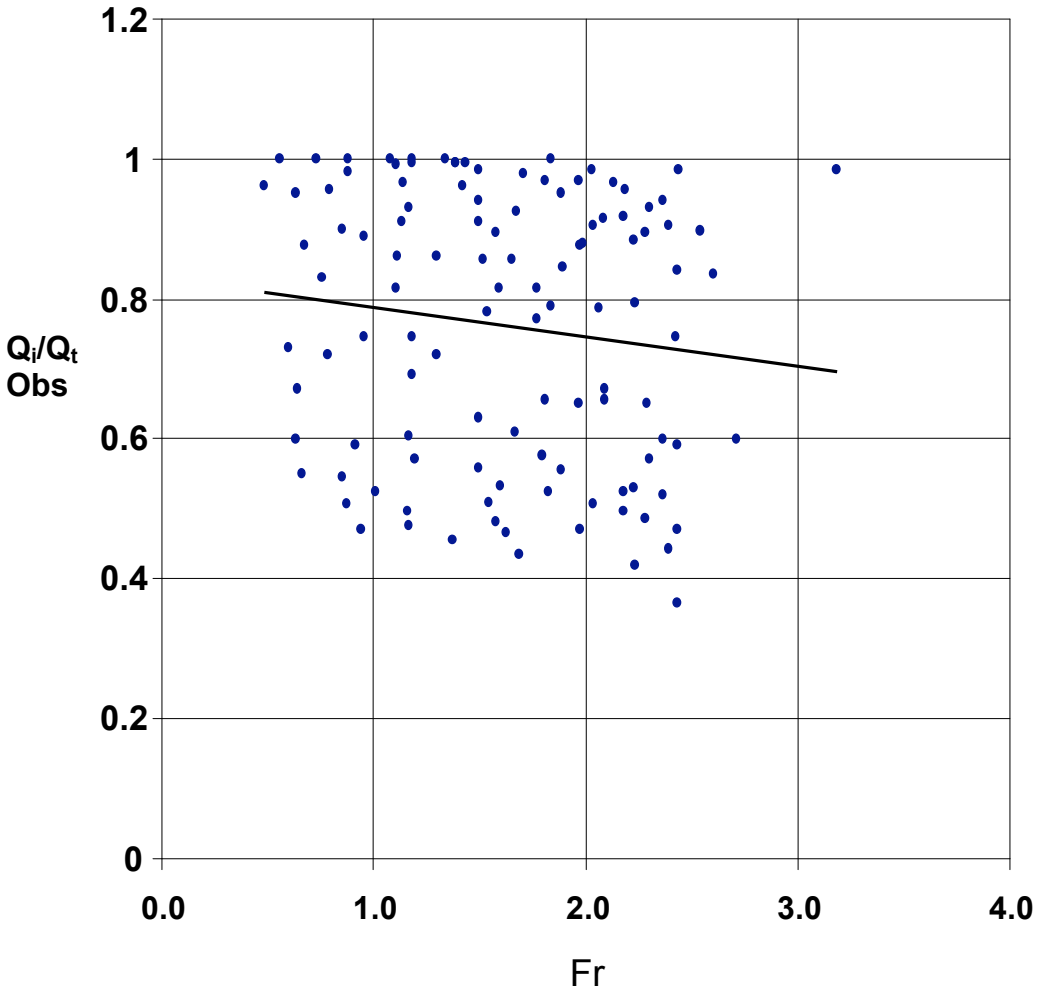

Figure 22. Plot of observed efficiency and Froude number with a linear trend line (CV 3-1/4).

In the figures 20-22 it could be observed that efficiency shows an inverse relation with Froude number. It is also evident that inspite of an inverse trend, for each Froude Number there are high efficiencies as well as low efficiencies recorded.

4.4 Flow depth calculations:

Because of cross slope of the flow channel, the cross section of flow is triangular and using the flow width, the depth of flow is calculated using simple geometry.

Figure 23 demonstrates the calculation of flow depth for a cross slope of 1 in 24, given the spread width. D' is the maximum flow depth above the channel bed, for computational purposes, mean depth D above the inlet is taken as two thirds of the maximum depth D'.

From the available graphs, values of total flow volume, observed hydraulic efficiency, width of flow and slope were extracted and tabulated. Dimensions and structural details of each of the inlets were available and were used to calculate the area of openings in each inlet which was required in obtaining effective area ratio which is one of the four explanatory variables to be used in the model.

4.5 The Proposed Models:

The proposed models were based on the postulation that the four non-dimensional variables: the longitudinal aspect ratio of inlet, the longitudinal slope of the channel, the effective area ratio of the inlet and the Froude number, are capable of defining the hydraulic efficiency of the inlet to a reasonable extent. The following two regression models were proposed:

Model 1: Additive terms model

Hydraulic Efficiency

$$\frac{Q_i}{Q_t} = \gamma_1 [W/L]^{\beta_1} + \gamma_2 [slope]^{\beta_2} + \gamma_3 [a_o / a_i]^{\beta_3} + \gamma_4 [Fr]^{\beta_4}$$

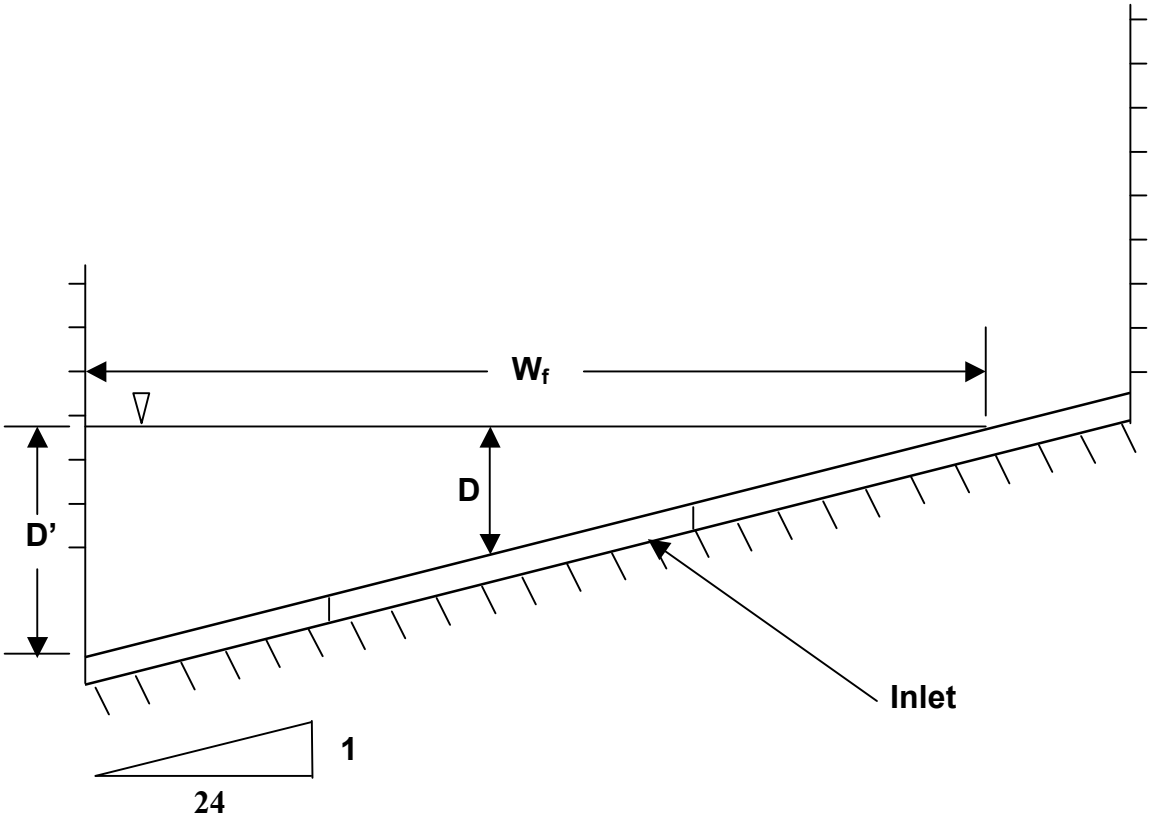

Figure 23. Cross section of the flow channel.

Model 2: Power Law Model

Hydraulic Efficiency

$$\frac{Q_i}{Q_t} = \gamma[W/L]^{\beta_1}[slope]^{\beta_2}[a_o / a_i]^{\beta_3}[Fr]^{\beta_4}$$

where,

W = Width of Inlet

L = Length of Inlet

W_f = Width of Flow

a_o/a_i = Effective Area Ratio of the Inlet

Q_t = Total Flow Volume

Q_i = Volume Intercepted by Inlet

Fr = Froude Number

At this stage experimental data for all variables in the above model and the observed efficiency corresponding to these data are available. The aim is to obtain the values of the parameters γ, γ_1, γ_2, γ_3, γ_4, β_1, β_2, β_3 and β_4 such that the resulting equation should predict efficiency in each respective equation. The consistency of the model can be verified by comparison of calculated efficiency values to the observed efficiency values. The solver function in excel spreadsheet was used to estimate the parameters using the method of least squares. Each type of the above mentioned inlet produced different values of parameters of the efficiency models, these parameters are listed in Table 3.

Table 3. Efficiency model 1 and the parameters corresponding to the three inlets.

Model 1: Additive								
$\frac{Q_i}{Q_t} = \gamma_1[W/L]^{\beta_1} + \gamma_2[slope]^{\beta_2} + \gamma_3[a_o/a_i]^{\beta_3} + \gamma_4[Fr]^{\beta_4}$								
Inlet	γ_1	β_1	γ_2	β_2	γ_3	β_3	γ_4	β_4
P 1-1/8	6.4538	0.056	0.011	0.106	0.00	-10.58	-5.52944	0.004
P 1-7/8	-13.1630	0.001	-2.44	-0.021	11.88	1.37	9.27533	-0.03604
CV 3-1/4	-0.0001	-9.93	-2.54	-0.040	2.86	0.80	2.28	-0.111

Table 4. Efficiency model 2 and the parameters corresponding to the three inlets.

Model 2: Power Law					
$\frac{Q_i}{Q_t} = \gamma[W/L]^{\beta_1}[slope]^{\beta_2}[a_o/a_i]^{\beta_3}[Fr]^{\beta_4}$					
Inlet	γ	β_1	β_2	β_3	β_4
P 1-1/8	10.0288	0.959	-0.008	2.90	-0.01
P 1-7/8	88.671	-0.0196	0.064	-0.44	12.74927
CV 3-1/4	1.750	0.091	0.057	-0.23	1.13

It can be observed that each parameter in a model fails to show consistency when compared to its counterpart in the other model. For example if we compare values of any one parameter, say β_1 from each model and go on comparing other parameters, there is no apparent pattern which can explain the effect of type of

inlet on the efficiency. Had there been a pattern in variation of these parameters, a concept of "shape factor" could have been possibly thought of which would have introduced a common "shape factor parameter" in each of these models and there would have been a unique model for all inlets with a shape factor associated with each of the types. Nevertheless, each of the above models proves to be quite consistent in computing efficiencies for its type.

The next chapter analyzes these models, their practical significance and, by comparing the calculated and observed values of hydraulic efficiency, also verify the consistencies of the models.

Chapter 5

Results

In chapter 4, two different statistical models (additive and power-law) were presented which were developed using literature reported data; three different types of inlets produced three models each representing the type from which it was developed. This chapter focuses on analyzing the consistency of the models by comparing the calculated and observed values of efficiencies. Further a comparison between observed and predicted values of efficiencies of a different inlet (in experiments carried out differently) is presented.

5.1 Additive Models

P 1- 1/8

The proposed model for P 1-7/8 inlet is given below and the corresponding parameters are given in Table 5.

$$\frac{Q_i}{Q_t} = \gamma_1 [W/L]^{\beta_1} + \gamma_2 [slope]^{\beta_2} + \gamma_3 [a_o / a_i]^{\beta_3} + \gamma_4 [Fr]^{\beta_4}$$

Table 5. Parameters for P1-1/8 Additive Model.

γ_1	β_1	γ_2	β_2	γ_3	β_3	γ_4	β_4
6.4540	0.056	0.027	0.108	0.00	-10.58	-5.53084	0.004

Figure 24 shows the comparison of observed and calculated values of hydraulic efficiency using the P 1- 7/8 inlet data. Comparing the calculated and observed values of hydraulic efficiency for the model the R-squared value is 0.6356

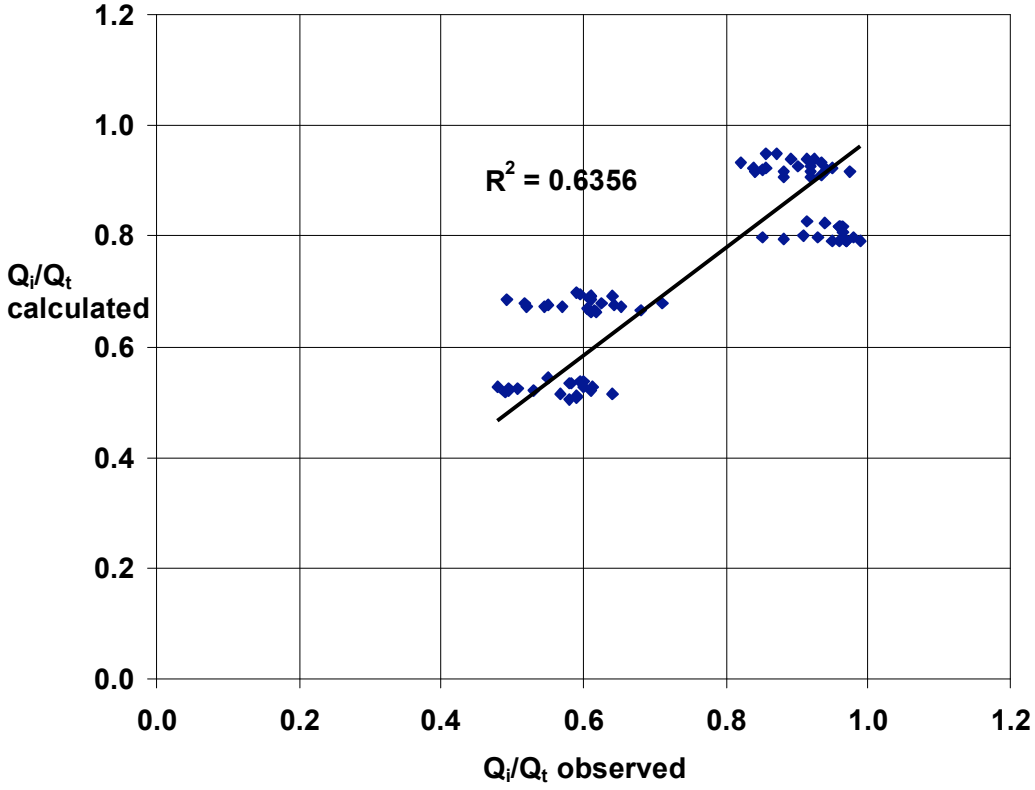

Figure 24. Evaluating the consistency of P 1-1/8 additive model, observed versus calculated efficiencies.

P 1- 7/8

The proposed model for P 1-7/8 inlet is given below and the corresponding parameters are given in Table 6.

$$\frac{Q_i}{Q_t} = \gamma_1[W/L]^{\beta_1} + \gamma_2[slope]^{\beta_2} + \gamma_3[a_o/a_i]^{\beta_3} + \gamma_4[Fr]^{\beta_4}$$

Table 6. Parameters for P1-7/8 Additive Model.

γ_1	β_1	γ_2	β_2	γ_3	β_3	γ_4	β_4
-13.163	0.001	-2.449	-0.021	11.88	1.37	9.275	-0.0360

Figure 25 shows the comparison of observed and calculated values of hydraulic efficiency using the P 1- 7/8 inlet data. Comparing the calculated and observed values of hydraulic efficiency for the model the R-squared value is 0.9433

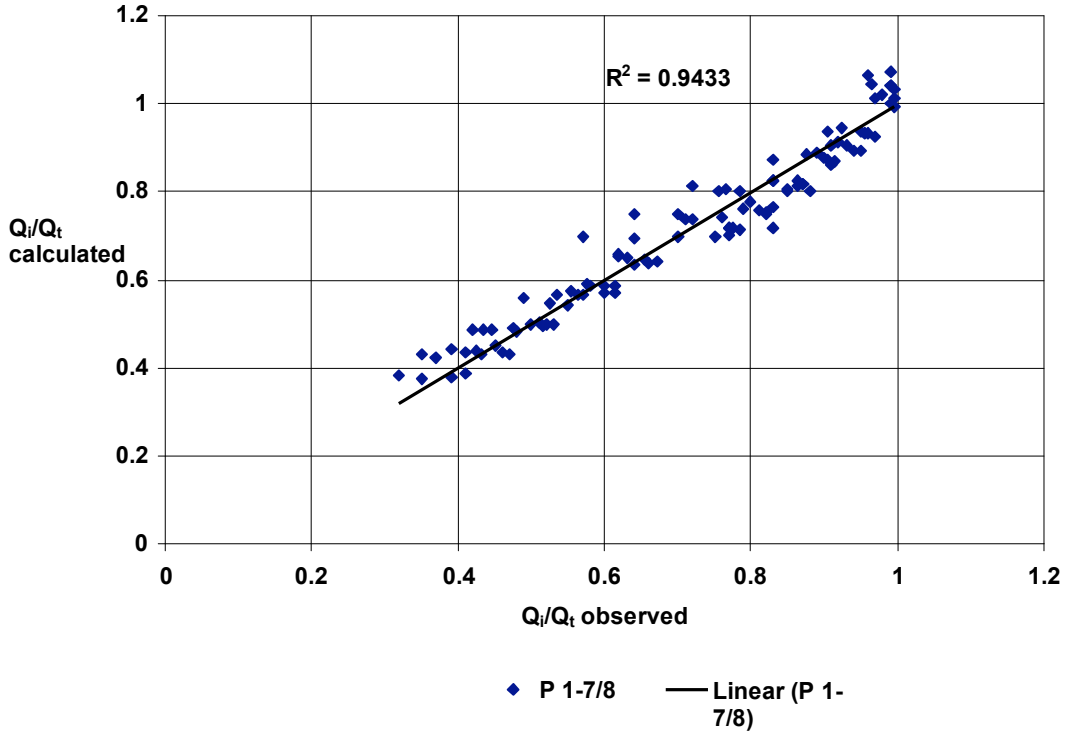

Figure 25. Evaluating the consistency of P 1-7/8 additive model, observed versus calculated efficiencies.

CV 3-1/4

The proposed model for CV 3-1/4 inlet is given below and the corresponding parameters are given in Table 7.

$$\frac{Q_i}{Q_t} = \gamma_1 [W/L]^{\beta_1} + \gamma_2 [slope]^{\beta_2} + \gamma_3 [a_o / a_i]^{\beta_3} + \gamma_4 [Fr]^{\beta_4}$$

Table 7. Parameters for CV 3-1/4 Additive Model.

γ_1	β_1	γ_2	β_2	γ_3	β_3	γ_4	β_4
-0.0001	-9.93	-2.547	-0.040	2.86	0.80	2.28	-0.111

Figure 26 shows the comparison of observed and calculated values of hydraulic efficiency using the CV 3-1/4 inlet data. Comparing the calculated and observed values of hydraulic efficiency for the model the R-squared value is 0.8238

5.2 Power Law Models

P 1- 1/8:

The proposed model for this type of inlet is given below and the corresponding parameters are given in Table 8.

$$\frac{Q_i}{Q_t} = \gamma [W/L]^{\beta_1} [slope]^{\beta_2} [a_o / a_i]^{\beta_3} [Fr]^{\beta_4}$$

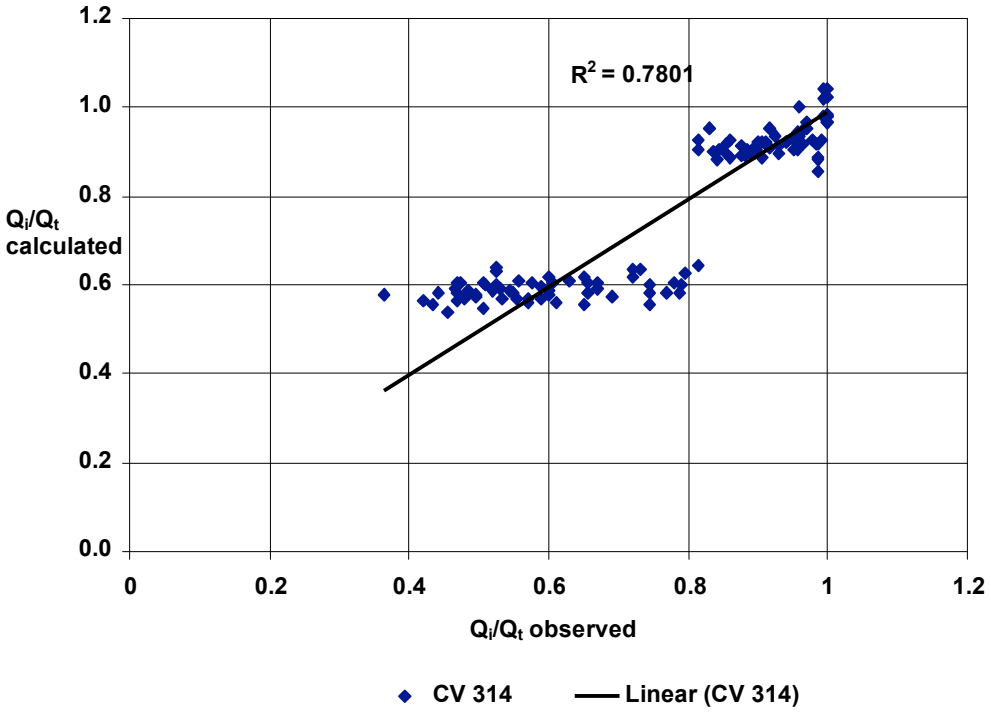

Figure 26. Evaluating the consistency of CV 3-1/4 additive model, observed versus calculated efficiencies.

Table 8. Parameters for P 1-1/8 Power Law Model.

γ	β1	β2	β3	β4
10.0288	0.959	-0.008	2.90	-0.01

Figure 27 shows the comparison of observed and calculated values of hydraulic efficiency using the P 1- 1/8 inlet data. Comparing the calculated and observed values of hydraulic efficiency for the model the R-squared value is 0.4543

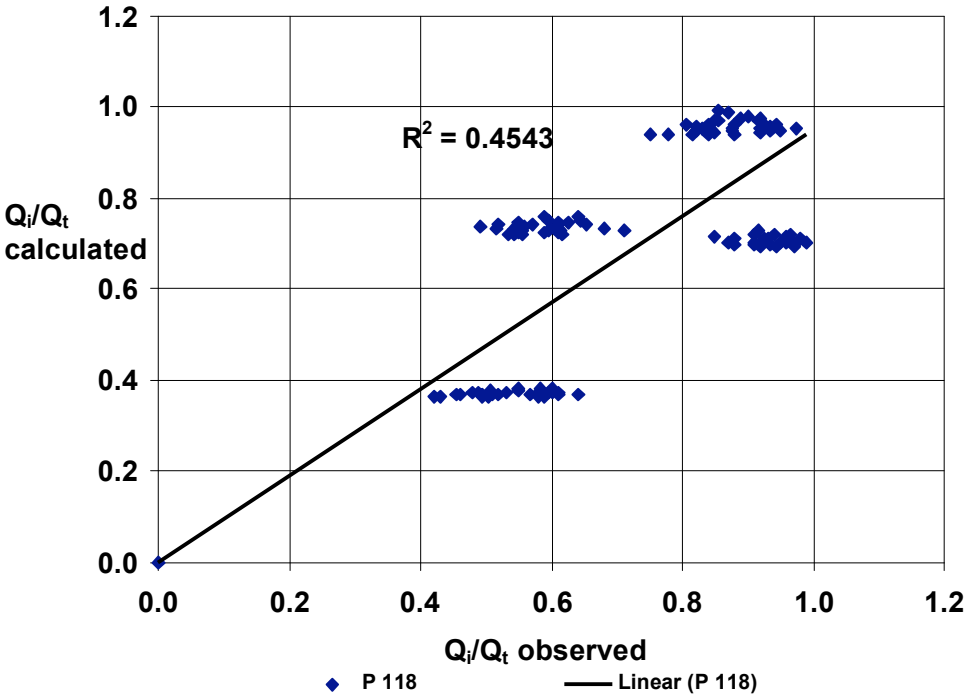

Figure 27. Evaluating the consistency of P 1-1/8 power law model, observed versus calculated efficiencies.

P 1- 7/8:

The proposed model for this type of inlet is given below and the corresponding parameters are given in Table 9.

$$\frac{Q_i}{Q_t} = \gamma [W/L]^{\beta_1} [slope]^{\beta_2} [a_o / a_i]^{\beta_3} [Fr]^{\beta_4}$$

Table 9. Parameters for P 1-7/8 Power Law Model.

γ	β1	β2	β3	β4
169.2454	-0.017	-0.102	13.49	0.220599

Figure 28 shows the comparison of observed and calculated values of hydraulic efficiency using the P 1- 7/8 inlet data. Comparing the calculated and observed values of hydraulic efficiency for the model the R-squared value is 0.5283

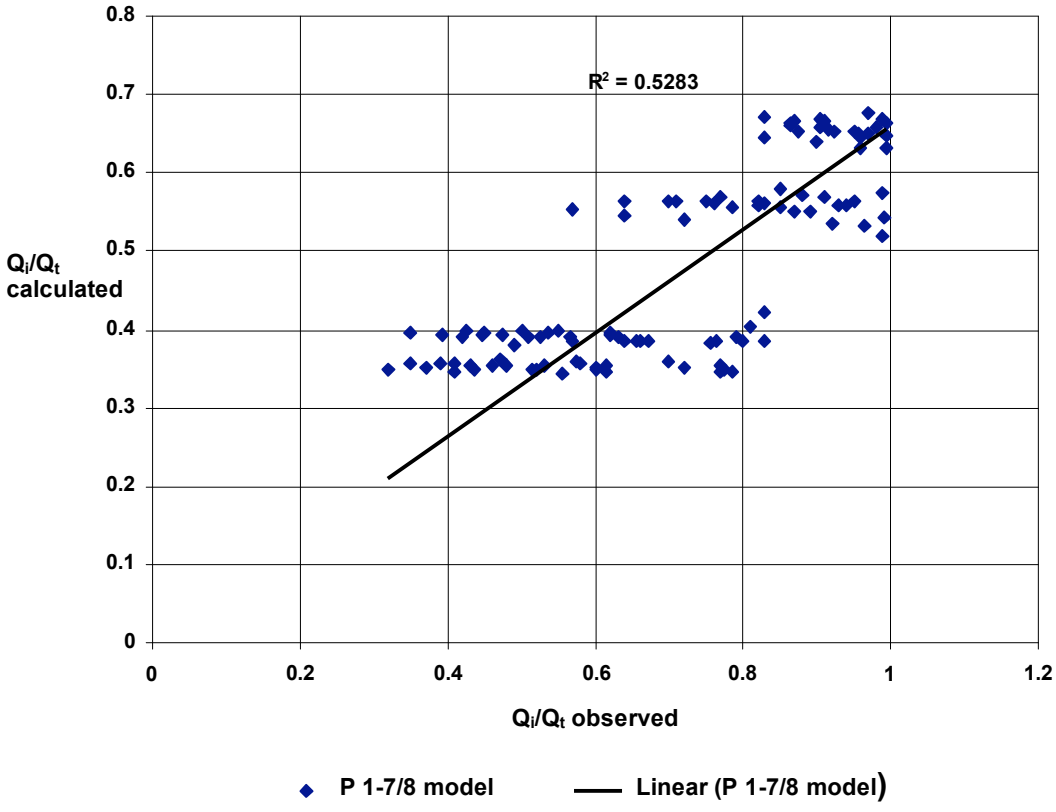

Figure 28. Evaluating the consistency of P 1-7/8 Power Law Model, observed versus calculated efficiencies.

P CV 3-1/4

The proposed model for this type of inlet is given below and the corresponding parameters are given in Table 10.

$$\frac{Q_i}{Q_t} = \gamma [W/L]^{\beta_1} [slope]^{\beta_2} [a_o / a_i]^{\beta_3} [Fr]^{\beta_4}$$

Table 10. Parameters for P 1-1/8 Power Law Model.

γ	β1	β2	β3	β4
1.750	0.091	0.057	-0.23	1.13

Figure 29 shows the comparison of observed and calculated values of hydraulic efficiency using the CV 3-1/4 inlet data. Comparing the calculated and observed values of hydraulic efficiency for the model the R-squared value is 0.7731

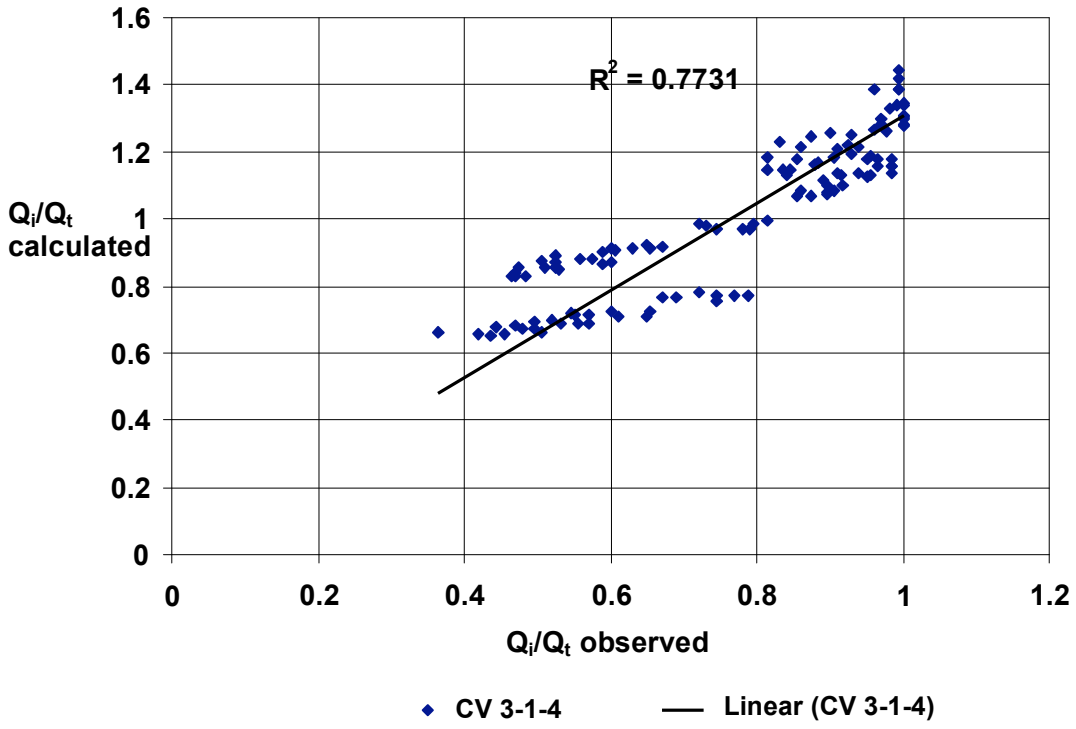

Figure 29. Evaluating the consistency of CV 3-1/4 Power Law Model, observed versus calculated efficiencies.

5.3 Testing the Models

The statistical models have been developed from the experimental data where it was clearly observed that the hydraulic efficiency varies inversely as the flow volume and it falls at steeper slopes. Data analysis showed that the shape and configuration of each inlet has an effect on the interception capacity of the inlet. The explanatory variables (effective area ratio and longitudinal aspect ratio) were chosen such that the effect of shape could be quantified in terms of their contribution to the efficiency. However the models could not be accepted as

consistent if they are compared to the same data from which they were generated. To verify the prediction consistency of the models, they are tried for a completely different set of data.

Experiments done by Woo and Jones (1974) involved different inlets tested for efficiency at varying longitudinal slopes and approach flow volumes. The models were used to predict efficiency values for these experiments and the predicted and observed values were compared. Given data enabled calculations of the variables used in the proposed model (i.e. longitudinal aspect ratio, effective area ratio and Froude number). Comparison of model calculated efficiency values and the observed values tabulated in the report produced graphs (each for power law and additive model) are shown in figure 30 and 31 respectively.

The CV 3-1/4 model was used to predict the efficiency values for an inlet type "TB45" (Woo and Jones, 1974) which is an inlet with cross bars tilted at 45 degree. The selection of CV 3-1/4 model for this type of inlet was owing to the structural similarity between curved vane inlet and tilted bar inlet. Both additive and power law models were used to calculate the efficiencies.

The power law model produced an R-squared value of 0.7751 and the additive model produced R-squared value of 0.7241

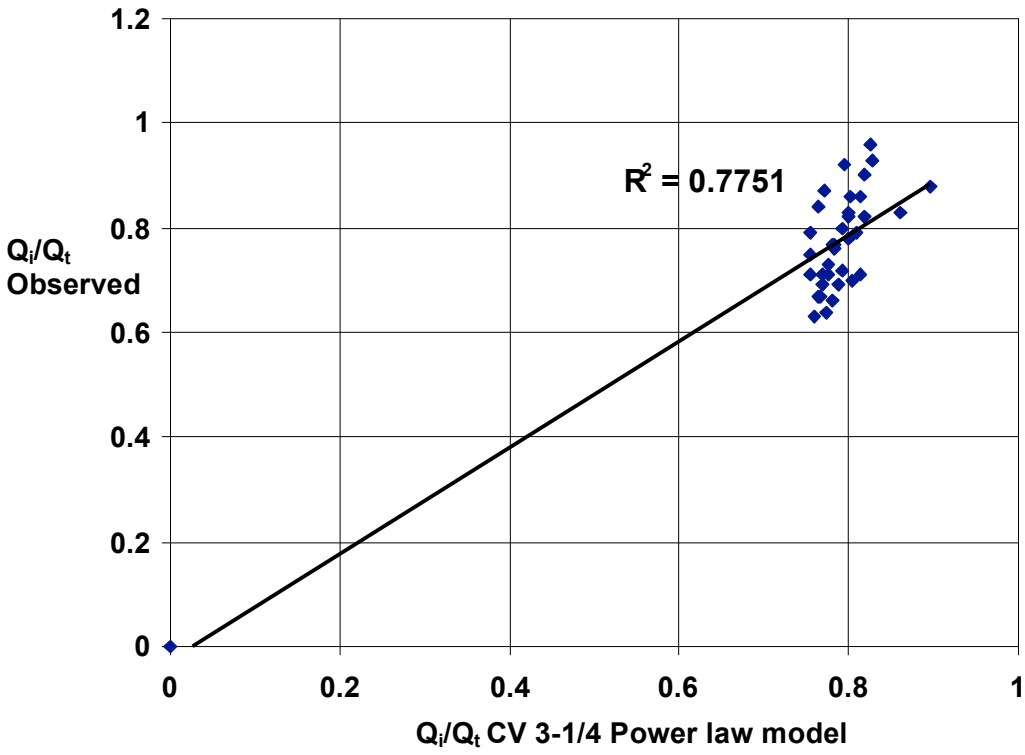

Figure 30. Using CV 3-1/4 power law model to calculate efficiency of TB45 type inlet.

The data against which the consistency of the CV 3-1/4 model has been tested are limited, low efficiency values are not available and in addition to it in spite of similar structure of the two inlets there is quite a difference between the way each inlet intercepts the inflow. In the curved vane inlet the vanes of the inlet emerge up from the plane of the inlet whereas in the tilted bar inlet the cross bars remain in the plane of inlet hence, for similar conditions a curved vane inlet is able to intercept greater amount of inflow volume. Because of these reasons the model predicts efficiency values which are slightly higher than the observed values.

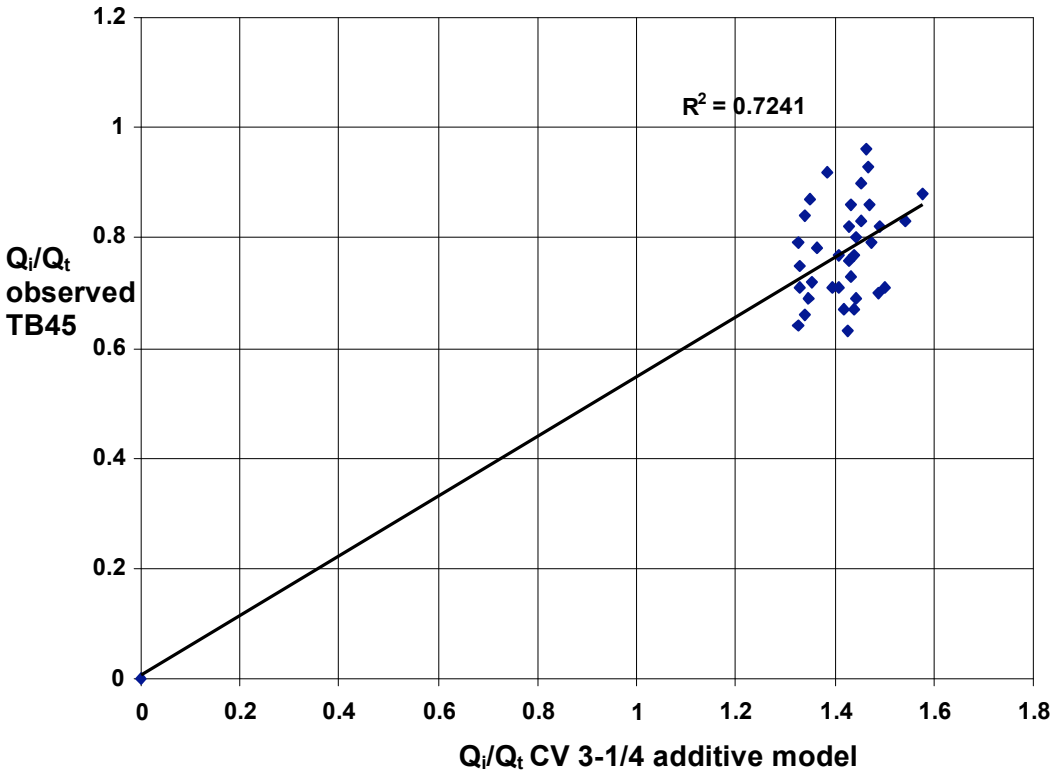

Figure 31. Using CV 3-1/4 additive model to calculate efficiency of TB45 type inlet.

5.4 Standard Errors and Prediction Error Bounds

The regressions were re-run in R 2.3.1 (R Development Core Team, 2006) to determine the standard errors, adjusted R-squared values associated with each of the models and the zone of uncertainty was quantified using the quantiles function. The results have been included in the Appendix B. The upper and lower bounds of the predictions errors are shown by the graph in figure 32.

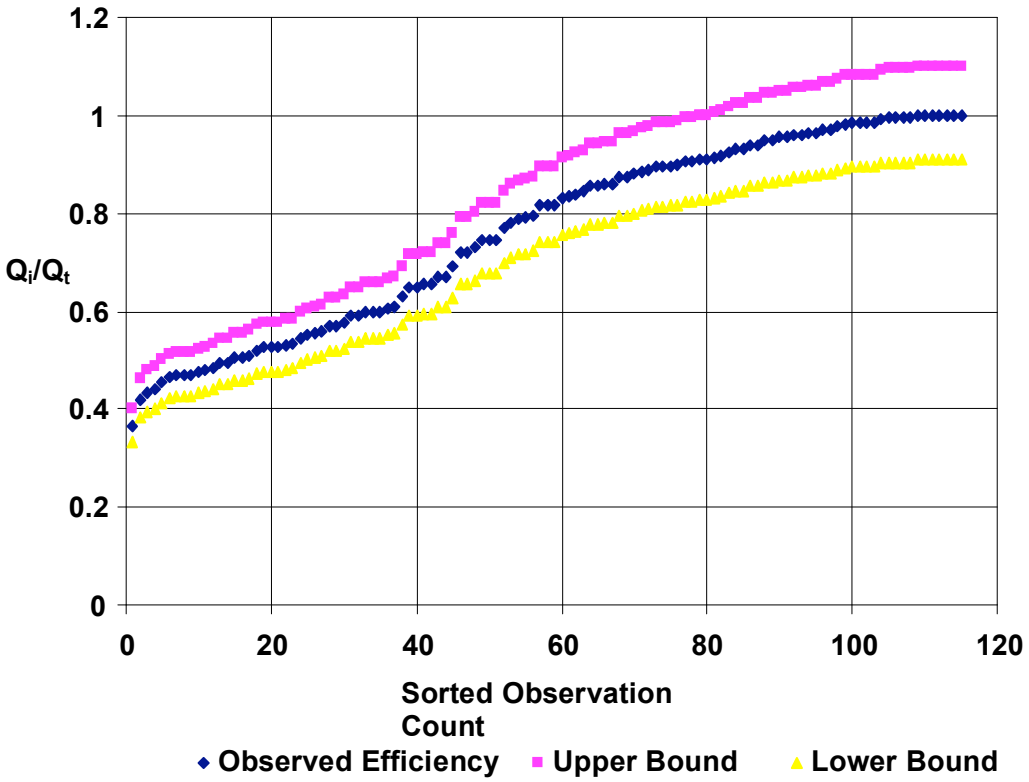

Figure 32. The prediction error bounds associated with the CV 3-1/4 power law model.

Chapter 6

Conclusions and Future Work

6.1 Design Oriented Experimental setup

The literature review found that the principal knowledge gaps are behavior in low slope (and backwater) conditions, debris handling behavior and series (cascade) inlets interactions.

Low slope behavior has not been well explained although the Florida DOT (Kranc, 2000) studies certainly considered low slope conditions. Debris problem with grate inlets has never been resolved; no successful experimental setups to simulate actual debris have been reported. The concept of "Self Cleaning Conditions" which is based on the idea of accelerating the approach flow just close to the inlet to increase the velocity so as to achieve self cleaning and getting rid of debris accumulation hasn't been analyzed.

No experiments have been found which collectively study an assembly of inlets in series. This particular type of study would be a step ahead in an attempt to simulate the actual conditions rather closely. This type of experiment, even if conducted at small scale (including violating Froude and Reynolds scaling) would be of great benefit in understanding what added benefit of a series of inlets could provide when a single inlet does not have sufficient capacity.

The present thesis is mainly based on data analysis, listed below are some important approaches which have not been addressed because of the absence of experimental data.

1. Developing flow fractions (efficiencies) over a realistic range of slopes for Texas applications.
2. Interpretation of results into dimensionless results if possible. Dimensionless forms would be beneficial for future researchers and designers as specifications evolve over time. While the current Type-H inlets are geometrically prescribed, a dimensionless representation would be of value in special cases where geometries need to be slightly adjusted.
3. Conducting a reasonable number of studies in low slope situations.
4. Induce backwater effects (ponding) in the inlets if possible.
5. Study cascades of inlets (if at all possible). In a practical sense these will by necessity be small scale models to calibrate CFD codes. Large-scale physical models of cascades (series) of inlets are currently impractical.
6. Examine debris handling.

The equations produced for estimating the hydraulic efficiencies of inlets using non-dimensional explanatory variables are necessarily statistical models or mathematical correlations in view of the fact that hydraulic efficiency doesn't share a physical relationship with the variables which are used for efficiency predictions.

In the previous chapter the statistical models were tested for different experiments and the equation produced intuitively expected results. The models thus prove to be on the right track if not perfectly correct.

R-squared values can not be takes as the best measure to scale the reliability of the model; the standard errors associated with each of the models (Appendix B) define the zone of uncertainty in the predictions of the statistical models. The approach or the limited data could be the reason for the failure to produce a unique statistical model which could predict efficiency for any inlet irrespective of its type. Comprehensive experimental data could improve the models and help in moving towards the goal of framing a 'type-independent' relation between non-dimensional explanatory variables and hydraulic efficiency.

Nevertheless these correlations can be used effectively to guide future experiments and also aid the design procedure for practical use of inlets. The models suggest efficiency computation based on measurements of flow volume, cross and longitudinal slopes, inlet dimensions and flow width. The results can be utilized for design of other intake structures like curb inlets.

Future experiments with wider range of longitudinal and cross slopes, zero slope and high flow conditions could be used to test the models further and improve them so as to narrow down the zone of uncertainty associated with the predictions. Behavior of inlet in backwater conditions and in ponding states can be expected to have interesting effects on the efficiency considering the fact that

in backwater conditions the approach velocity of the inflow would be reduced considerably, thereby giving itself more time for interception. Further, cascaded system of inlet would be another test for these statistical models. The variations in values of parameters with change in the number of inlets in series (simulating actual field conditions) would be an important data to modify the co-relations. A cascaded system of inlets with partial ponding is also a practical scenario which can be studied.

Detailed study of clogging of inlets due to debris would be required to modify the inlets so as to minimize clogging and it would be interesting to observe the effect on efficiency of the inlet after modification and the corresponding change in the effective area ratio of the inlet.

References

AASHTO Officials Select Committee on Highway Safety, "Highway Design and Operational Practices Related to Highway Safety, Second Edition." Washington, D.C.,
1974.

ASCE, (1993). Design and Construction of Urban Stormwater Management System, ASCE New York. 700 p.

Brown S.A, S.M. Stein, J.C. Warner (2001). Urban Drainage Design Manual Hydraulic Engineering Circular 22, Second Edition Federal Highway Administration, Hydraulic Engineering Circular, HEC22 FHWA-NHI-01-021, U.S. Department of Transportation, Washington, D.C., 478p.

Burgi, P H; Gober, D E (1978a) HYDRAULIC AND SAFETY CHARACTERISTICS OF SELECTED GRATE INLETS. ABRIDGMENT.TRB Research Record No. 685, Geometrics, Hydraulics, and Hydrology.

Burgi, P. H., (1978b). Bicycle-Safe Grate Inlets Study, Volume-2 Hydraulic Characteristics of Three Selected Grate Inlets on Continuous Grades, Federal Highway Administration Report No. FHWA-RD-78-4

Burgi, P. H., (1978c). Bicycle-Safe Grate Inlets Study, Volume-3 Hydraulic Characteristics of Three Selected Grate Inlets in a Sump Condition, Federal Highway Administration Report No. FHWA-RD-78-70.

Cassidy, J.J. (1966). Generalized Hydraulic Characteristics of Grate Inlets. Highway Research Board Record No. 123, Washington, D.C. pp. 36-48.

Johnson F. L. and Fred F.M. Chang (1984). Drainage of Highway Pavements, Federal Highway Administration, HEC No. 12 FHWA-TS-84-202.

Inlet Grate Capacities Manual [Electronic Version] Neenah Foundry Company, Test Program to Determine Inlet Grate Capacities for Gutter Flow. Retrieved February 12 2007 from
http://www.nfco.com/literature/brochures/gratecapacities.html

Kranc, S.C., (2000). Hydraulic performance of several curb and gutter inlets. Final Report BB-895. Florida Department of Transportation.

Kranc, S.C., and Anderson, M.W., (1993). Investigation of discharge through grated inlets. Report No. 611. Florida Department of Transportation, Office of Research Management. 32p.

Larson, C.L., (1947). Investigation of Flow Through Standard and Experimental Grate Inlets for Street Gutters, University of Minnesota St. Anthony Falls Hydraulic Laboratory. Project Report No. 3.

Larson, C.L., (1948). Experiments on Flow Through Inlet Gratings for Street Gutters. Highway Research Board Research Report 6-B, Washington D.C., pp 17-29.

McEnroe B.M., Reuben P. Wade and Andrew K. Smith (1999). HYDRAULIC PERFORMANCE OF CURB AND GUTTER INLETS.K-TRAN: KU-99-1. Kansas Department of Transportation.

R Development Core Team (2006). R: A language and environment for statistical computing. R Foundation for Statistical Computing,Vienna, Austria. ISBN 3-90-0051-07-0, URL http://www.R-project.org.

Texas Department of Transportation, (2004). "Hydraulic Design Manual." Austin, TX, (available at ftp://ftp.dot.state.tx.us/pub/txdot-info/gsd/manuals/hyd.pdf

Thompson, D.B., Fang, X., Gharty-Chhetri Om Bahadur (2004). SYNTHESIS OF TxDOT STORM DRAIN DESIGN. Report 0-4553-1, Texas Department of Transportation.

Transportation Research Board, (1969). "Traffic-Safe and Hydraulically Efficient Drainage Practices," NCHRP Synthesis of Highway Practice 3, TRC, Washington, D.C.

Wisconsin Department of Transportation (1997). Facilities Development Manual Chapter 13 Section 25 Subject 30 Bureau of Highway Development, Procedure 13-25-30.

Woo, D.C., Jones, J. S., (1974). Hydraulic Characteristics of Two Bicycle-Safe Grate Inlet Designs. Report FHWA-RD-74-77 (Final Report), Federal Highway Administration, U.S. Department of Transportation, Washington, D.C.

Appendix A

Structural details of the inlets

One of the explanatory variables requires computing area of openings in an inlet. Details of the three different types of inlets (Burgi, 1978) are given below. The drawings below have been developed based on the details given in FHWA report on "Bicycle safe grate inlets, vol.2 by Burgi P. H.

A.1

P 1-1/8 Type Inlet:

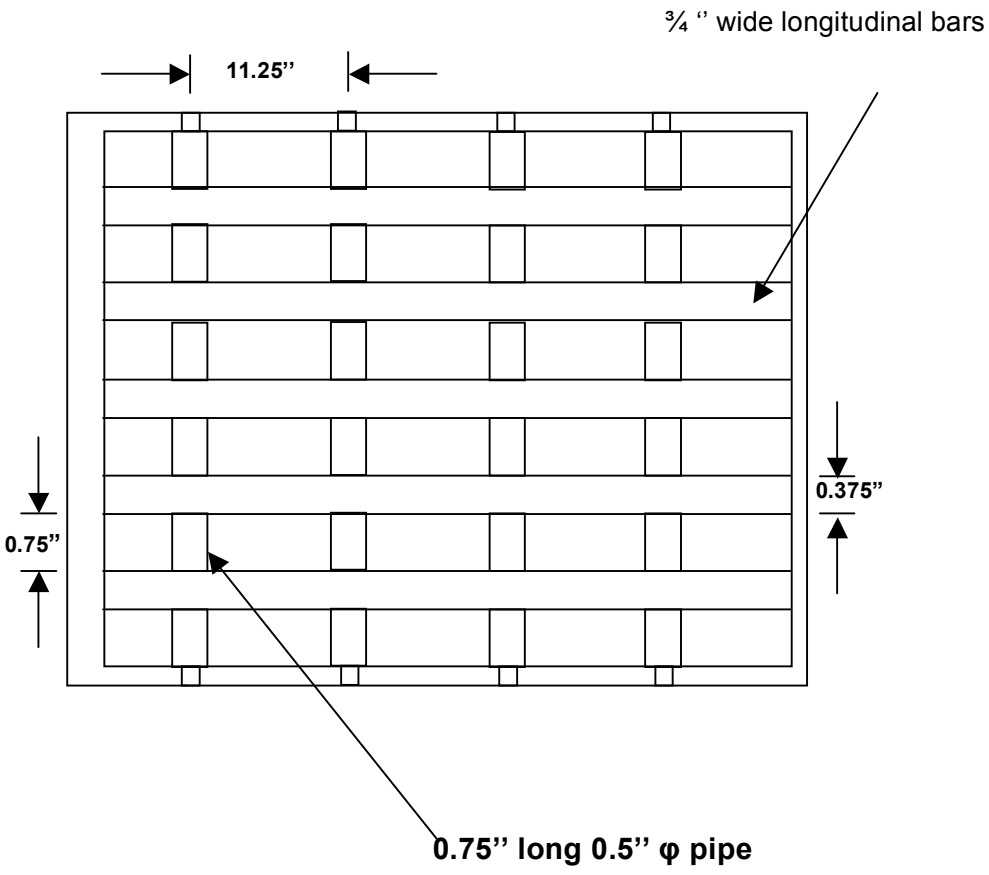

Figure A1. Details of the P 1-1/8 type inlet.

A.2

P 1-7/8 Type Inlet:

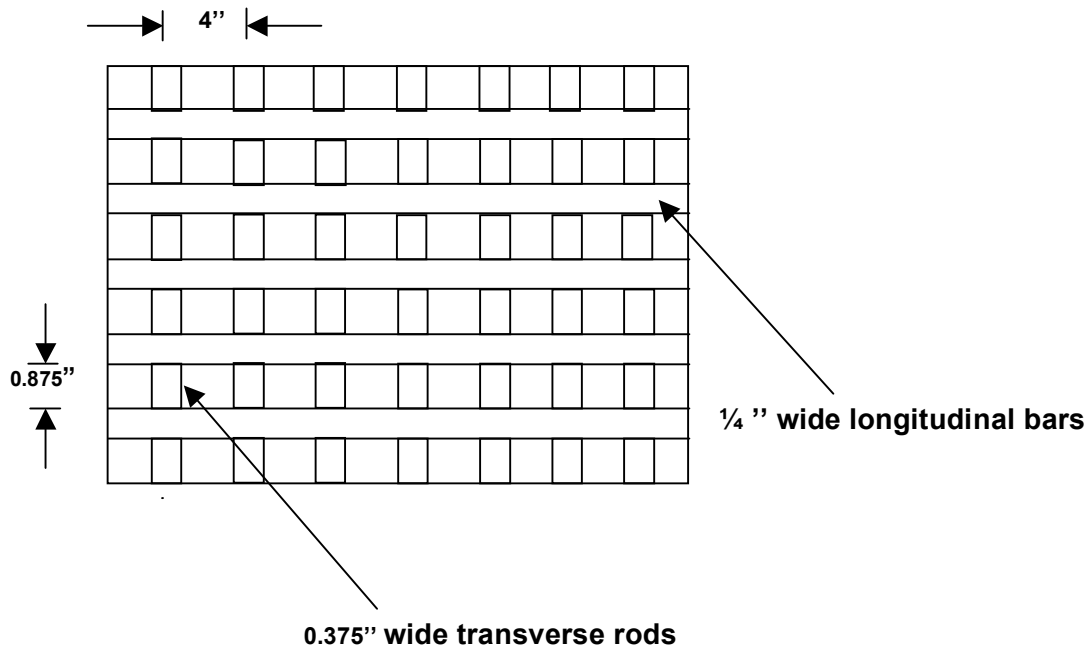

Figure A2. Details of the P 1-7/8 type inlet.

A.3

CV 3-1/4 Type Inlet:

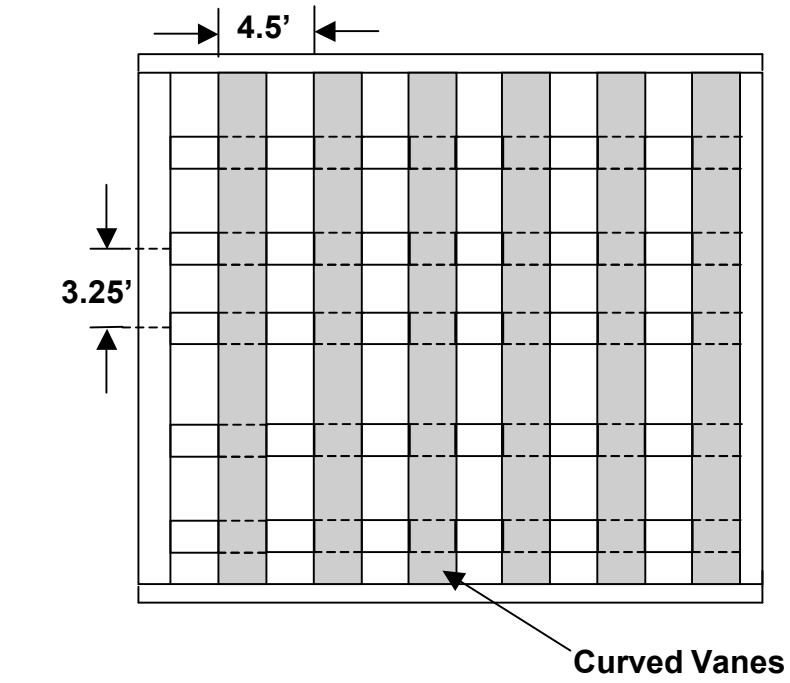

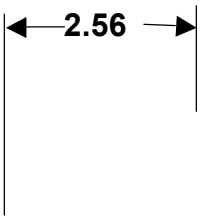

Curved vane

Figure A3. Details of the curved vane type of inlet (CV 3-1/4).

Appendix B

Regressions with R-console

Regressions of the models plotted in R-console and the corresponding adjusted R-squared values, standard errors and quantiles of the zone of uncertainty have been reproduced in this appendix. Both the additive and power law models have been included.

B.1 Additive Models

P 1-1/8 additive model

```
Residuals:
     Min       1Q   Median       3Q      Max
-0.234178 -0.068951  0.005363  0.069262  0.254763

Coefficients:
            Estimate Std. Error t value Pr(>|t|)
(Intercept) -0.050949   0.078725  -0.647  0.51886
wratio       0.089207   0.030850   2.892  0.00462 **
slope        0.011482   0.005088   2.256  0.02602 *
aratio       2.922443   0.271882  10.749  < 2e-16 ***
fr          -0.092263   0.036417  -2.534  0.01270 *
---
Signif. codes:  0 '***' 0.001 '**' 0.01 '*' 0.05 '.' 0.1 ' ' 1

Residual standard error: 0.1069 on 110 degrees of freedom
Multiple R-Squared: 0.7037,     Adjusted R-squared: 0.693
F-statistic: 65.33 on 4 and 110 DF,  p-value: < 2.2e-16

quantile(resid(fit1),probs=c(0.025,0.05,0.1,0.2,0.3,0.4,0.5,0.6,0.7,0.8,0.9,0.95,0.9
75))
       2.5%          5%         10%         20%         30%         40%         50%
-0.206898970 -0.190759784 -0.140772476 -0.086846137 -0.055040257 -
0.019361792  0.005362591
        60%         70%         80%         90%         95%       97.5%
```

0.036480073 0.053158947 0.094817845 0.120040867 0.162375580
0.200512075

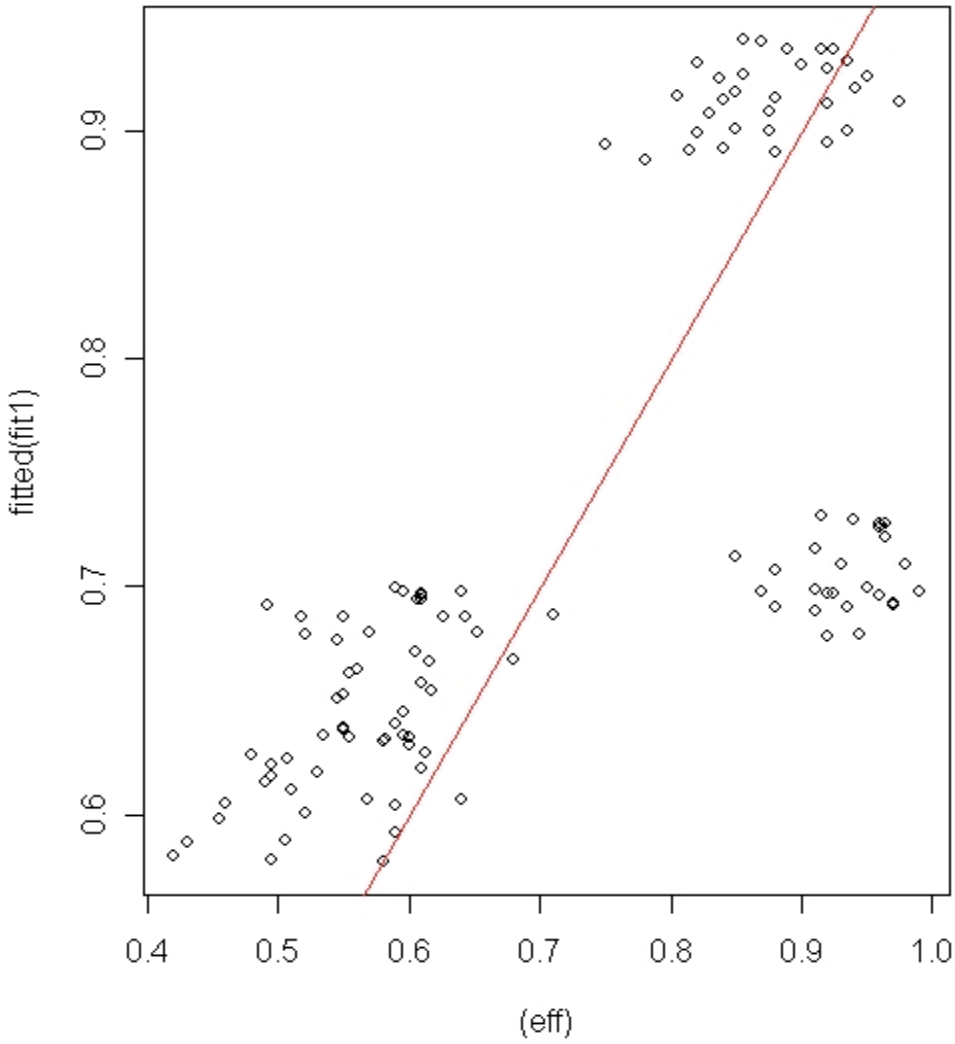

Figure B1. P 1-1/8 Additive Model regression in R-console.

P 1-7/8 additive model

```
Residuals:
    Min      1Q  Median      3Q     Max
-0.21860 -0.08325 -0.01745  0.07266  0.37163

Coefficients:
            Estimate Std. Error t value Pr(>|t|)
(Intercept) -7.385832   0.733166 -10.074   <2e-16 ***
wratio      -0.010116   0.035325  -0.286    0.775
slope        0.004368   0.007854   0.556    0.579
aratio      12.226012   1.109774  11.017   <2e-16 ***
fr          -0.085314   0.051986  -1.641    0.104
---
Signif. codes:  0 '***' 0.001 '**' 0.01 '*' 0.05 '.' 0.1 ' ' 1

Residual standard error: 0.1166 on 101 degrees of freedom
Multiple R-Squared: 0.6624,     Adjusted R-squared: 0.649
F-statistic: 49.54 on 4 and 101 DF,  p-value: < 2.2e-16

>
quantile(resid(fit1),probs=c(0.025,0.05,0.1,0.2,0.3,0.4,0.5,0.6,0.7,0.8,0.9,0.95,0.9
75))

2.5%         5%        10%        20%        30%        40%        50%        60%      70%
80%

-0.17900122 -0.15478648 -0.13340130 -0.09940931 -0.07045670 -0.03817348 –

0.01744914  0.01951860  0.05492154  0.08273756

 90%        95%       97.5%

 0.13756757  0.21895652  0.25068860
```

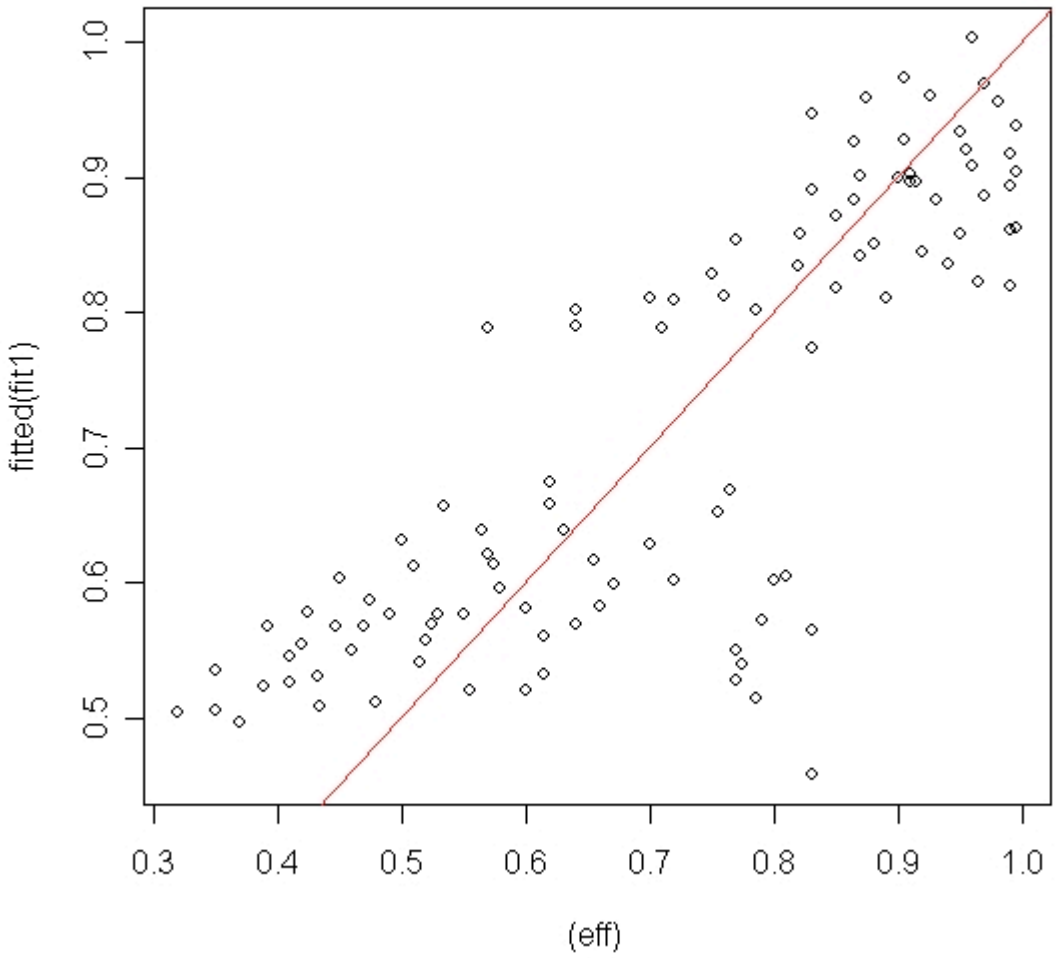

Figure B2. P 1-7/8 Additive Model regression in R-console.

CV 3-1/4 additive model

Residuals:

Min	1Q	Median	3Q	Max
-0.234178	-0.068951	0.005363	0.069262	0.254763

Coefficients:

	Estimate	Std. Error	t value	Pr(>|t|)	
(Intercept)	-0.050949	0.078725	-0.647	0.51886	
wratio	0.089207	0.030850	2.892	0.00462	**
slope	0.011482	0.005088	2.256	0.02602	*
aratio	2.922443	0.271882	10.749	< 2e-16	***
fr	-0.092263	0.036417	-2.534	0.01270	*

Signif. codes: 0 '***' 0.001 '**' 0.01 '*' 0.05 '.' 0.1 ' ' 1

Residual standard error: 0.1069 on 110 degrees of freedom
Multiple R-Squared: 0.7037, Adjusted R-squared: 0.693
F-statistic: 65.33 on 4 and 110 DF, p-value: < 2.2e-16

>
quantile(resid(fit1),probs=c(0.025,0.05,0.1,0.2,0.3,0.4,0.5,0.6,0.7,0.8,0.9,0.95,0.975))

2.5%	5%	10%	20%	30%	40%	50%
-0.206898970	-0.190759784	-0.140772476	-0.086846137	-0.055040257	-0.019361792	0.005362591

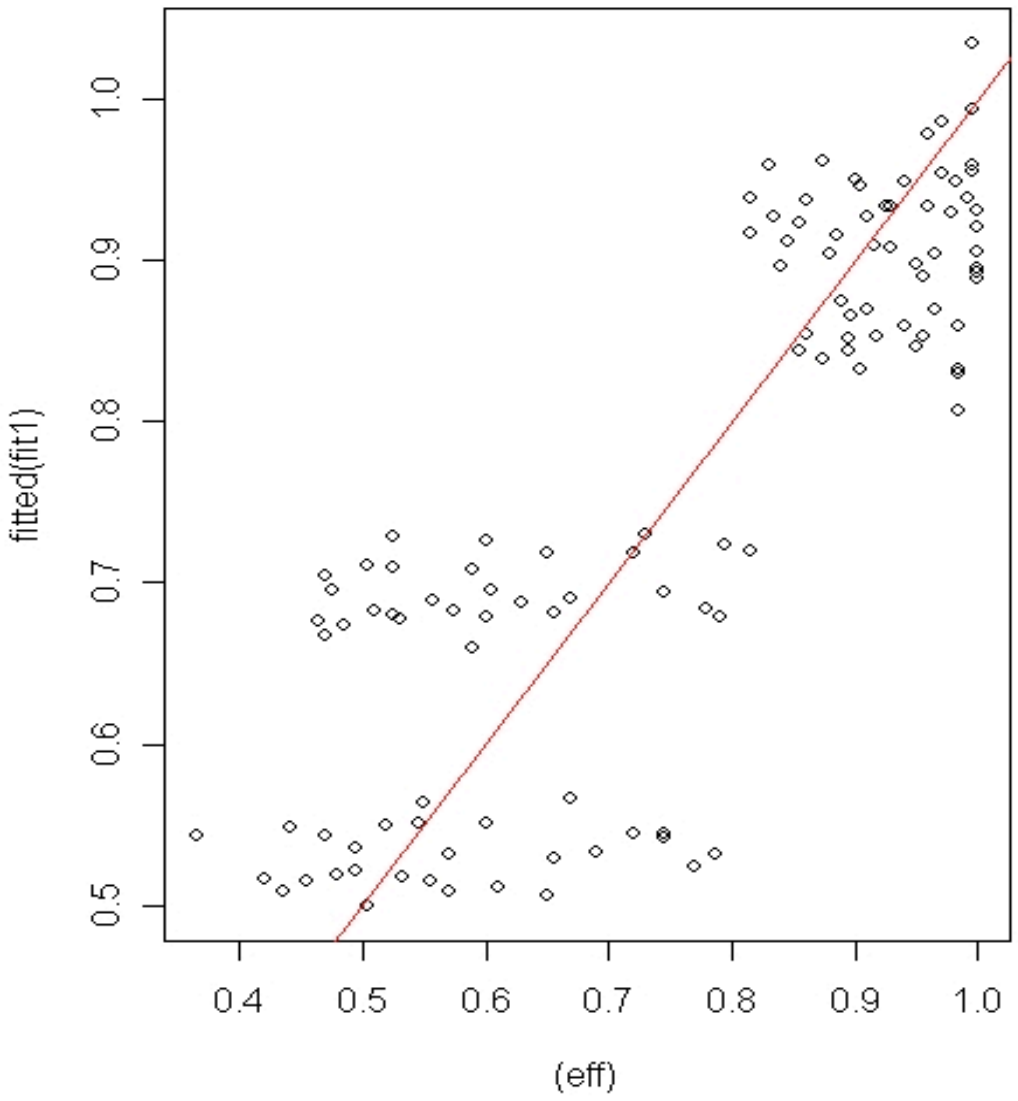

60%	70%	80%	90%	95%	97.5%
0.036480073	0.053158947	0.094817845	0.120040867	0.162375580	0.200512075

Figure B3. CV 3-1/4 Additive Model regression in R-console.

B.2 Power Law Models

P 1-1/8

```
Residuals:
     Min       1Q   Median       3Q      Max
-0.084029 -0.010419  0.001070  0.014370  0.123105

Coefficients: (1 not defined because of singularities)
              Estimate  Std. Error   t value  Pr(>|t|)
(Intercept)    0.199704   0.009895   20.182   < 2e-16  ***
log10(wratio) -0.137605   0.019654   -7.002   2.11e-10 ***
log10(slope)  -0.079799   0.006036  -13.221   < 2e-16  ***
log10(wfratio) 0.666084   0.020043   33.232   < 2e-16  ***
log10(aratio)        NA         NA       NA        NA
log10(flow)   -0.015776   0.009405   -1.677    0.0963 .
---

Signif. codes:  0 '***' 0.001 '**' 0.01 '*' 0.05 '.' 0.1 ' ' 1

Residual standard error: 0.02467 on 110 degrees of freedom
Multiple R-Squared: 0.9513,     Adjusted R-squared: 0.9495
F-statistic: 537.1 on 4 and 110 DF,  p-value: < 2.2e-16
```

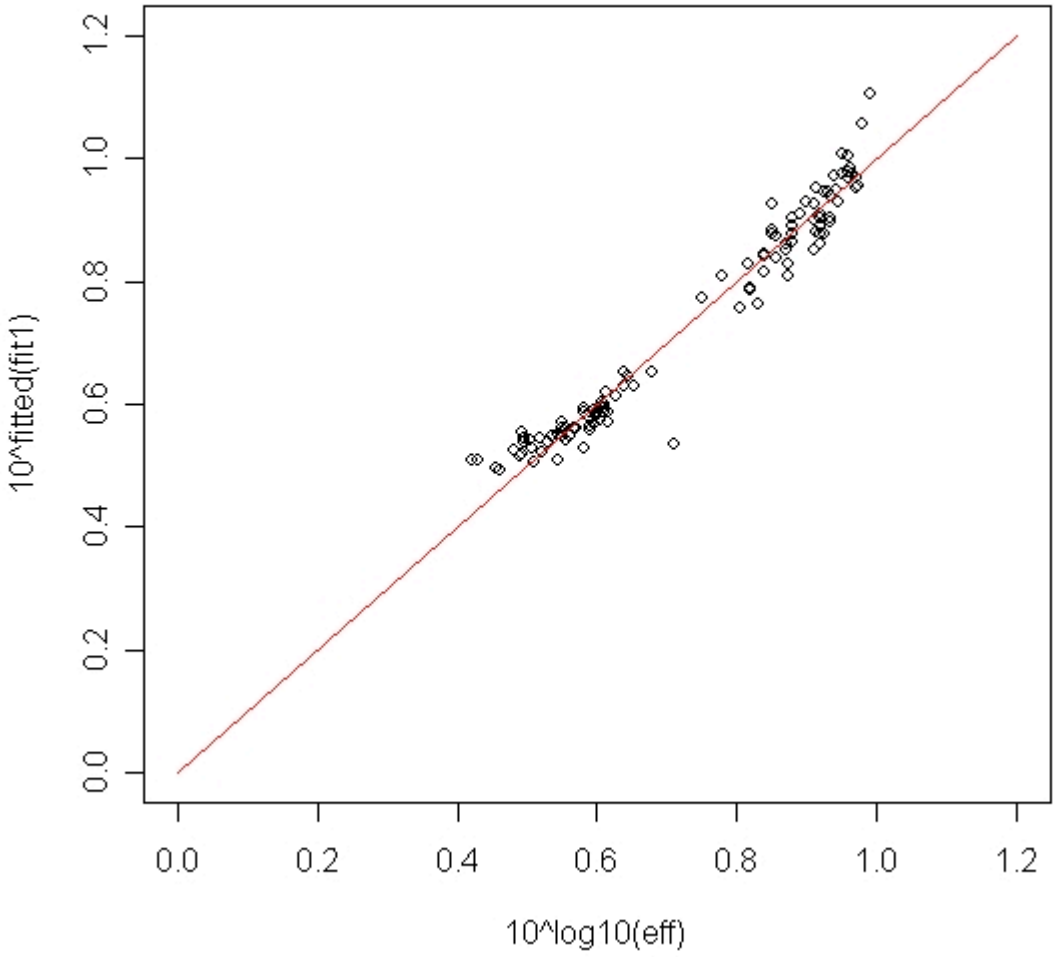

Figure B4. Regression in R 2.3.1 for P 1-1/8 model.

P 1-7/8

```
Residuals:
     Min       1Q   Median       3Q      Max
-0.109345 -0.022805  0.004152  0.029790  0.055857

Coefficients:
              Estimate Std. Error t value Pr(>|t|)
(Intercept)    1.01436    0.68577   1.479   0.1422
log10(wratio) -0.17052    0.07595  -2.245   0.0270 *
log10(slope)  -0.10844    0.04350  -2.493   0.0143 *
log10(aratio)  4.90787    4.49526   1.092   0.2775
log10(wfratio) 0.52466    0.24877   2.109   0.0374 *
log10(flow)   -0.13488    0.09673  -1.394   0.1663
---
Signif. codes:  0 '***' 0.001 '**' 0.01 '*' 0.05 '.' 0.1 ' ' 1

Residual standard error: 0.03684 on 100 degrees of freedom
Multiple R-Squared: 0.9254,     Adjusted R-squared: 0.9217
F-statistic: 248.3 on 5 and 100 DF,  p-value: < 2.2e-16
```

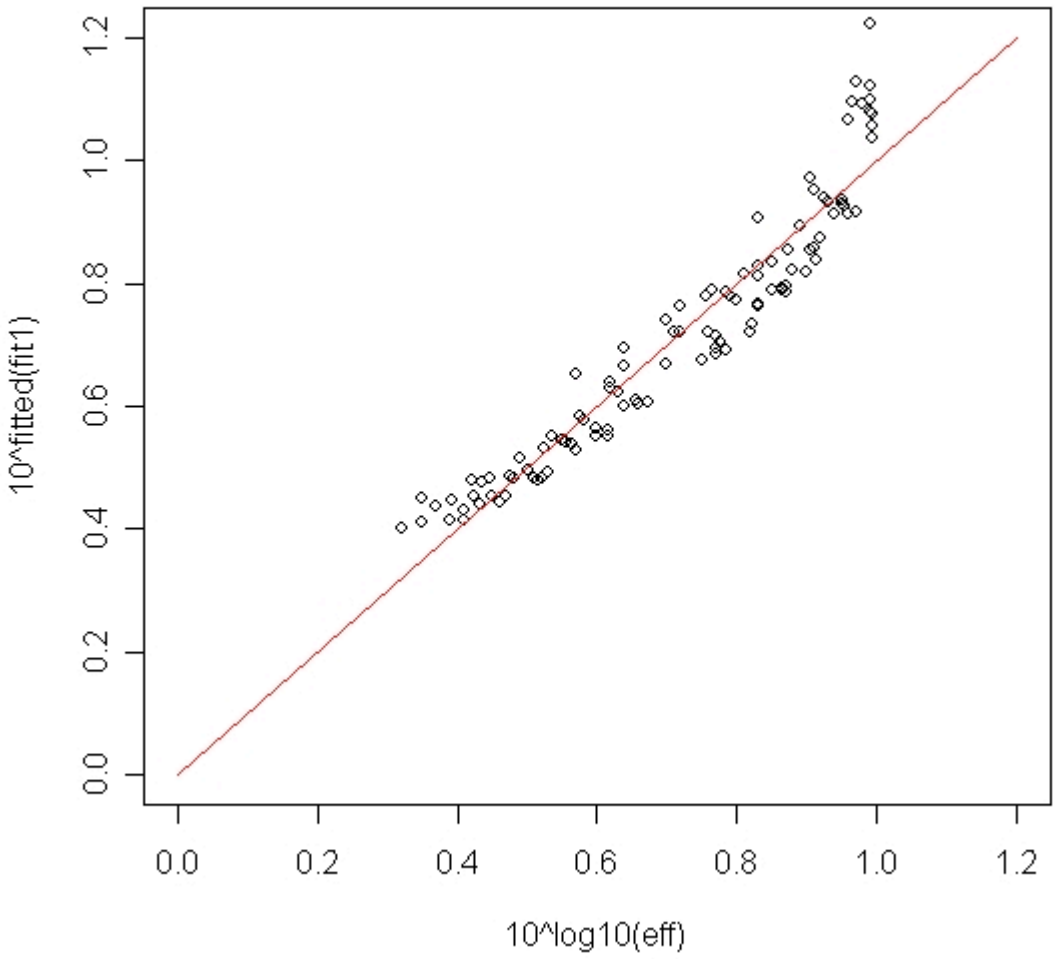

Figure B5. Regression in R 2.3.1 for P 1-7/8 model.

B.6

CV 3-1/4

Residuals:

```
    Min      1Q  Median      3Q     Max
-0.11902 -0.01659  0.00600  0.02070  0.05047

Coefficients:
                Estimate Std. Error t value Pr(>|t|)
(Intercept)     0.241687   0.030967   7.805 3.89e-12 ***
log10(wratio)  -0.052731   0.024583  -2.145  0.03417 *
log10(slope)   -0.052351   0.008931  -5.862 4.96e-08 ***
log10(aratio)   0.203061   0.072697   2.793  0.00617 **
log10(wfratio)  0.535864   0.038903  13.774  < 2e-16 ***
log10(flow)    -0.031324   0.017669  -1.773  0.07906 .
---
Signif. codes:  0 '***' 0.001 '**' 0.01 '*' 0.05 '.' 0.1 ' ' 1

Residual standard error: 0.02916 on 109 degrees of freedom
Multiple R-Squared: 0.9433,     Adjusted R-squared: 0.9407
F-statistic:   363 on 5 and 109 DF,  p-value: < 2.2e-16
```

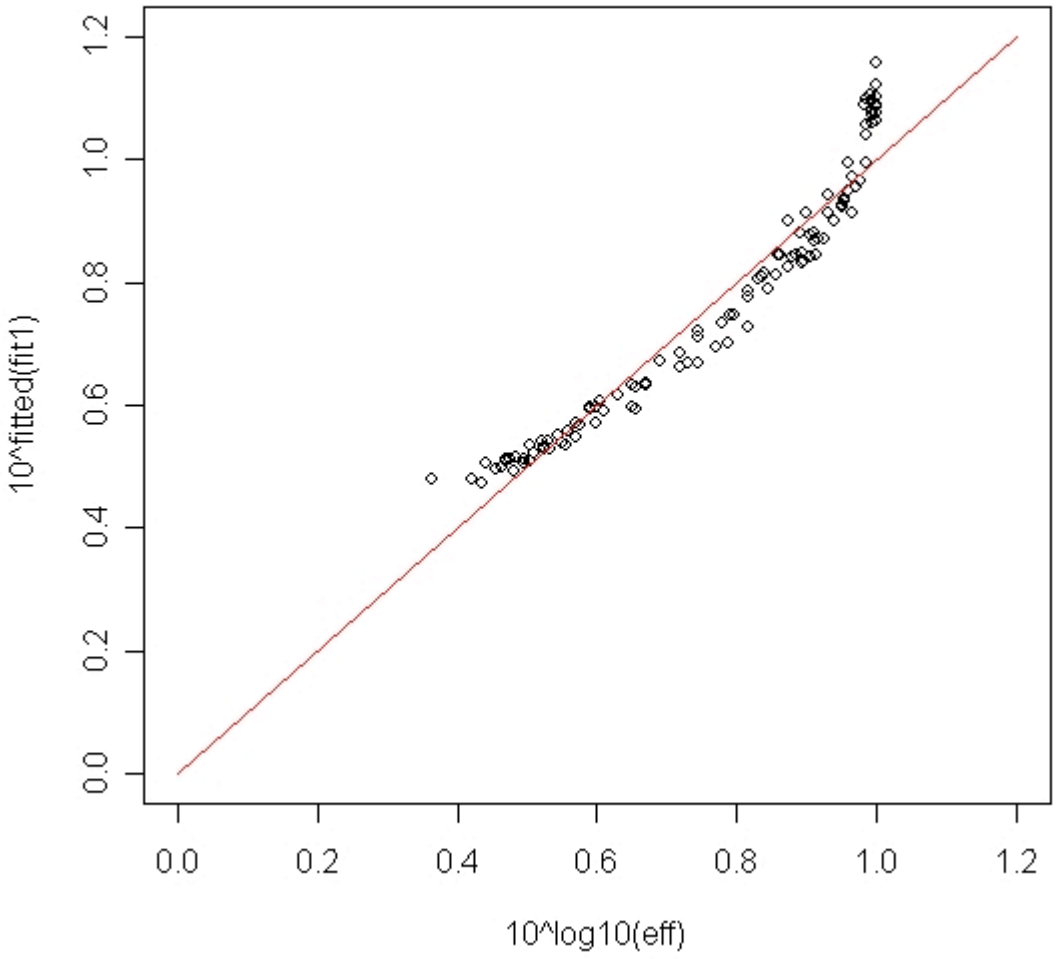

Figure B6. Regression in R 2.3.1 for CV 3-1/4 model.

Appendix C

Data tables for the use of CV 3-1/4 models in computing efficiencies for TB45-3 type model.

Table C1 shows the data adopted from Cassidy (1966) used to calculate the explanatory variables and use of the CV 3-1/4 additive model to compute the efficiency. Table C2 lists the corresponding parameters of the models.

Table C1. data adapted from Cassidy (1966) and use of CV 3-1/4 additive model to compute efficiency.

a_0/ai	W/L
0.5	0.896

Slope	Qt	depth	Fr	W_f	Q_i/Q_t observed	Q_i/Q_t calculated
					0	0
0.5	1.776	0.258	0.796465	3	0.78	1.3646656
0.5	2.19	0.288	0.832738	3	0.72	1.3530285
0.5	2.4	0.302	0.849873	3	0.69	1.347726
0.5	2.665	0.316	0.881698	3	0.66	1.3381856
0.5	2.926	0.326	0.923849	3	0.64	1.326123
1	1.244	0.178	0.973517	3	0.92	1.3846042
1	1.776	0.206	1.116337	3	0.87	1.3498104
1	1.98	0.216	1.159145	3	0.84	1.3403391
1	2.407	0.237	1.226046	3	0.79	1.32629
1	2.665	0.255	1.216298	3	0.75	1.3282832
1	2.926	0.272	1.2122	3	0.71	1.3291266
2.8	1.02	0.146	1.074544	3	0.96	1.4626747
2.8	1.245	0.169	1.053156	3	0.93	1.4677732
2.8	1.474	0.182	1.11569	3	0.9	1.4531762
2.8	1.776	0.195	1.212116	3	0.86	1.4323635
2.8	1.98	0.208	1.226658	3	0.82	1.4293852

2.8	2.4	0.223	1.33939	3	0.77	1.4075497
2.8	2.94	0.247	1.407522	3	0.71	1.395322
5.4	1.02	0.167	0.878372	3	0.88	1.577963
5.4	1.47	0.161	1.337309	3	0.86	1.4715801
5.4	1.776	0.173	1.450531	3	0.83	1.4515833
5.4	1.98	0.182	1.498688	3	0.8	1.4435981
5.4	2.4	0.199	1.588857	3	0.76	1.4293866
5.4	2.926	0.215	1.724924	3	0.71	1.4095565
7.5	1.02	0.14	1.144356	3	0.83	1.5416416
7.5	1.244	0.139	1.410754	3	0.82	1.4896138
7.5	1.47	0.149	1.502073	3	0.79	1.474257
7.5	1.98	0.165	1.736171	3	0.77	1.4392051
7.5	2.4	0.184	1.787054	3	0.73	1.432282
7.5	2.92	0.201	1.904329	3	0.67	1.4171272
13	1.02	0.109	1.665765	2.7	0.71	1.5005092
13	1.47	0.134	1.761219	3	0.7	1.4871126
13	1.98	0.144	2.129485	3	0.69	1.442086
13	2.407	0.162	2.169486	3	0.67	1.4377242
13	2.926	0.179	2.270638	3	0.63	1.4270815

Table C2. Parameters of CV 3-1/4 additive model.

γ_1	β_1	γ_2	β_2	γ_3	β_3	γ_4	β_4
-0.0001	-9.93	-2.547	-0.040	2.86	0.80	2.28	-0.111

$$\frac{Q_i}{Q_t} = \gamma_1 [W/L]^{\beta_1} + \gamma_2 [slope]^{\beta_2} + \gamma_3 [a_o / a_i]^{\beta_3} + \gamma_4 [Fr]^{\beta_4}$$

Table C3 shows the data adopted from Cassidy (1966) used to calculate the explanatory variables and use of the CV 3-1/4 power law model to compute the efficiency. Table C4 lists the corresponding parameters of the model.

Table C3. data adopted from Cassidy (1966) and use of CV 3-1/4 power law model to compute efficiency.

a_0/ai	W/L
0.5	0.896

Slope	Q_t	depth	W_f	FR	Q_i/Q_t observed	Q_i/Q_t calculated
					0	0
0.5	3.229	0.328	3	0.8082	0.78	0.799909
0.5	3.6	0.342	3	0.8463	0.72	0.791772
0.5	3.989	0.366	3	0.847	0.69	0.788079
0.5	4.376	0.384	3	0.8646	0.66	0.781456
0.5	4.845	0.401	3	0.8971	0.64	0.773123
0.5	5.319	0.414	3	0.9388	0.92	0.794898
1	2.262	0.226	3	0.9899	0.87	0.770306
1	3.229	0.261	3	1.1385	0.84	0.763681
1	3.6	0.274	3	1.1801	0.79	0.753906
1	4.376	0.301	3	1.2459	0.75	0.755289
1	4.845	0.324	3	1.2351	0.71	0.755875
1	3.319	0.345	3	0.7701	0.96	0.824405
2.8	1.845	0.185	3	1.0901	0.93	0.828219
2.8	2.263	0.214	3	1.0747	0.9	0.817324
2.8	2.68	0.231	3	1.1349	0.86	0.801918
2.8	3.229	0.248	3	1.2292	0.82	0.799725
2.8	3.6	0.264	3	1.2478	0.77	0.783746
2.8	4.363	0.284	3	1.3553	0.71	0.77487
2.8	5.345	0.314	3	1.4282	0.88	0.896632
5.4	1.854	0.212	3	0.893	0.86	0.814155
5.4	2.676	0.205	3	1.3555	0.83	0.799106
5.4	3.229	0.219	3	1.4813	0.8	0.793137
5.4	3.6	0.232	3	1.5147	0.76	0.78257
5.4	4.376	0.253	3	1.6167	0.71	0.767947

5.4	5.319	0.273	3	1.7532	0.83	0.85987
7.5	1.854	0.178	3	1.1607	0.82	0.819535
7.5	2.262	0.177	3	1.4282	0.79	0.80782
7.5	2.676	0.189	3	1.5312	0.77	0.781402
7.5	3.6	0.21	3	1.7588	0.73	0.776237
7.5	4.376	0.233	3	1.8293	0.67	0.764993
7.5	5.319	0.256	2.7	1.9307	0.71	0.814174
13	0.927	0.116	3	1.4265	0.7	0.803825
13	1.854	0.138	3	1.8482	0.69	0.769541
13	2.676	0.171	3	1.7792	0.67	0.76626
13	3.6	0.183	3	2.1621	0.63	0.758286
13	4.376	0.206	3	2.2005	0	0
13	5.319	0.228	3	2.2971	0.78	0.799909

Table C4. Parameters of the CV 3-1/4 power law model.

γ	β1	β2	β3	β4
1.75	0.09108	0.05741	-0.2295	1.1320

$$\frac{Q_i}{Q_t} = \gamma [W/L]^{\beta_1} [slope]^{\beta_2} [a_o / a_i]^{\beta_3} [Fr]^{\beta_4}$$